Nanospintronics using molecular nanomagnets

Wolfgang Wernsdorfer

Institut Néel, CNRS - Grenoble

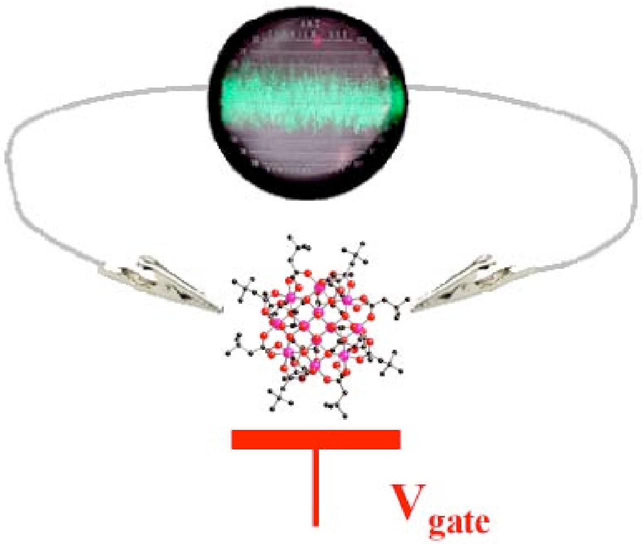

S = 1/2 to ≈ 40

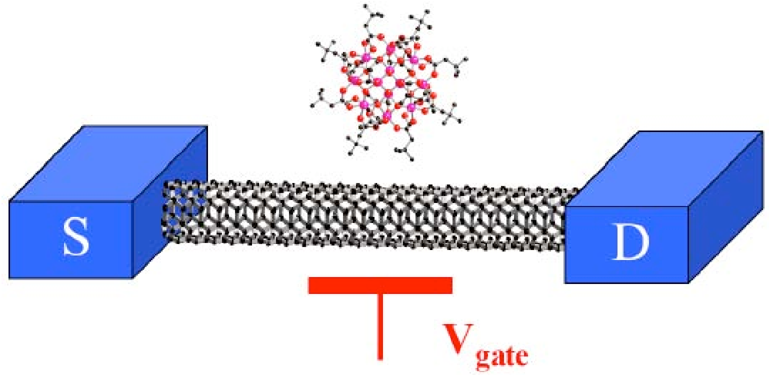

Magnetic structures

← *macroscopic* | *atomic* →

permanent magnets	micron particles	nanoparticles	clusters	molecular clusters	atoms

$S = 10^{20}$ 10^{10} 10^{8} 10^{6} 10^{5} 10^{4} 10^{3} 10^{2} 10 1

multi - domains ***single - domains*** ***spins***

1 mm

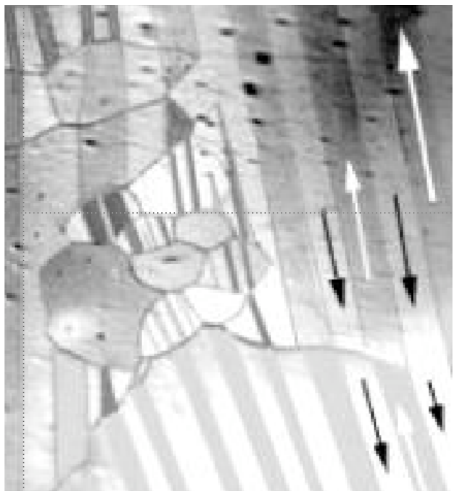

20 nm

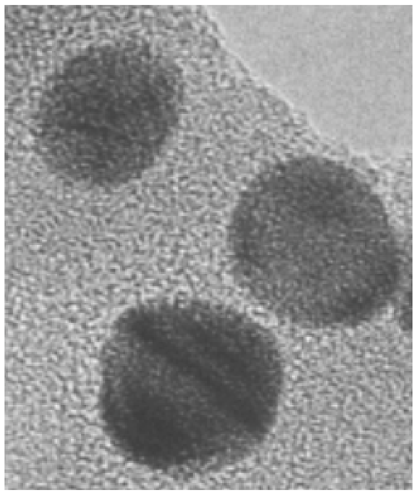

3 nm

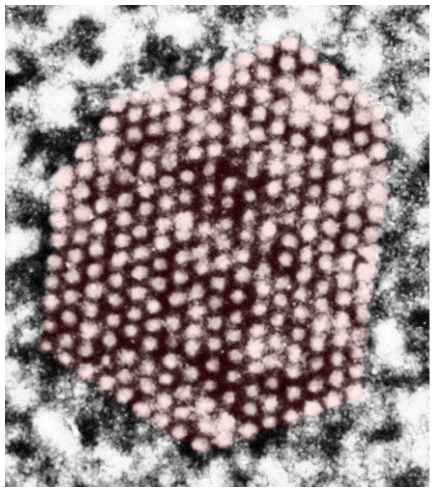

1 nm

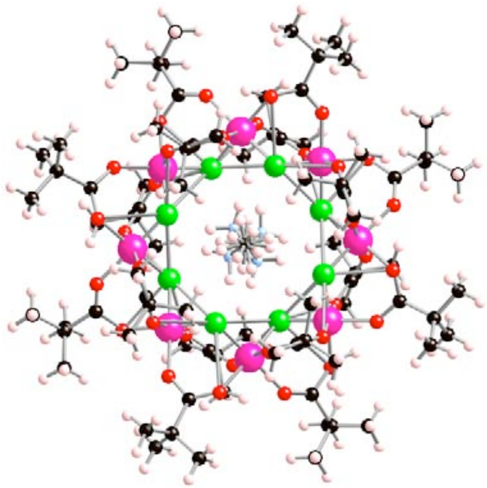

Micro-SQUID magnetometry

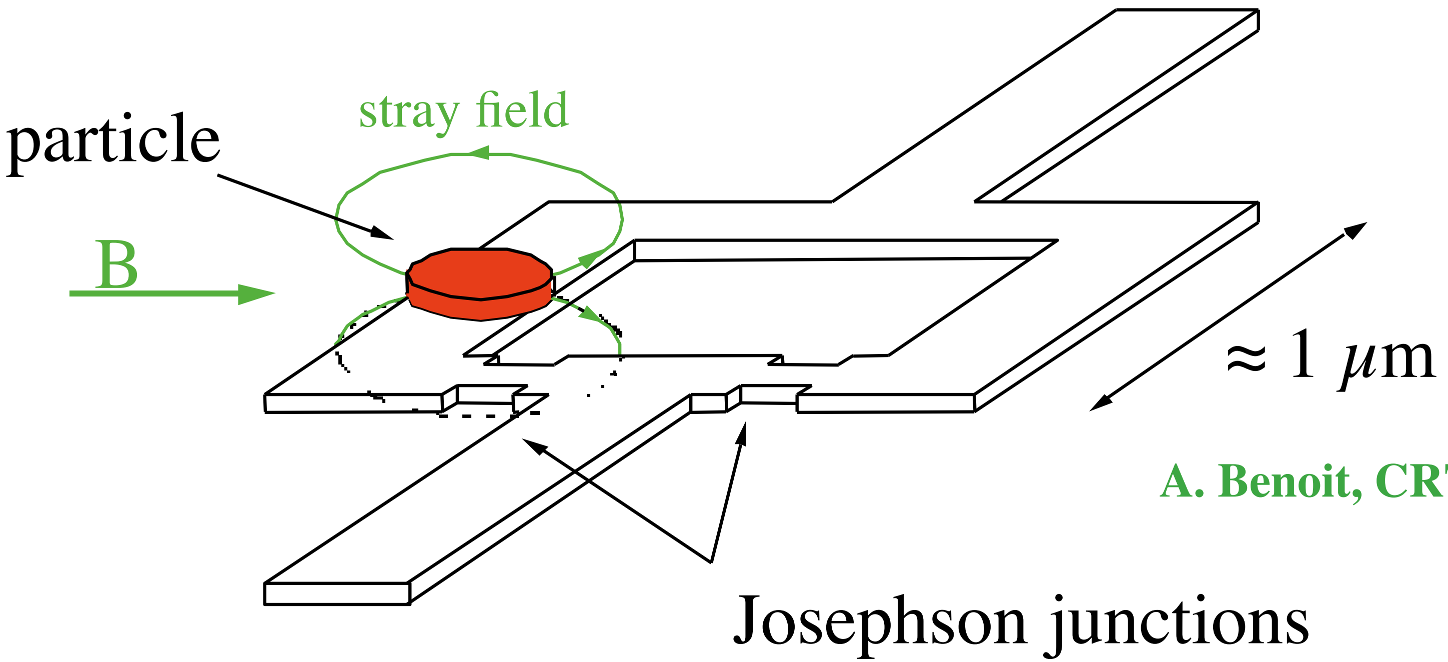

A. Benoit, CRTBT, 1989

- **fabricated by electron beam lithography**
  (D. Mailly, LPN, Marcoussis - Paris)

- **sensitivity : $10^{-4}\ \Phi_0$**
  ≈ $10^{2} - 10^{3}\ \mu_B$ i.e. $(2\ \mathrm{nm})^{3}$ of Co
  ≈ $10^{-18} - 10^{-17}$ emu

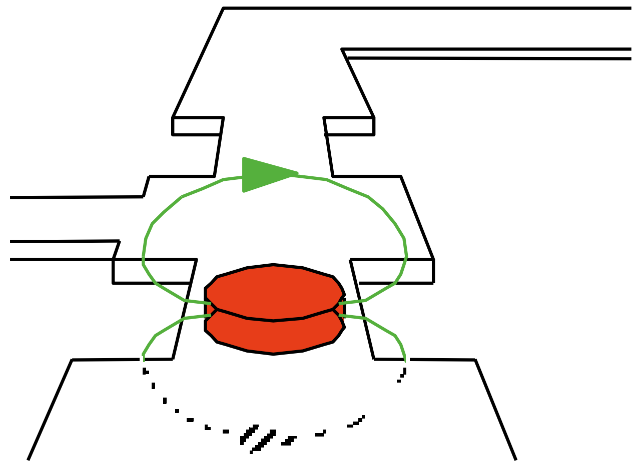

Roadmap of the micro-SQUID technique

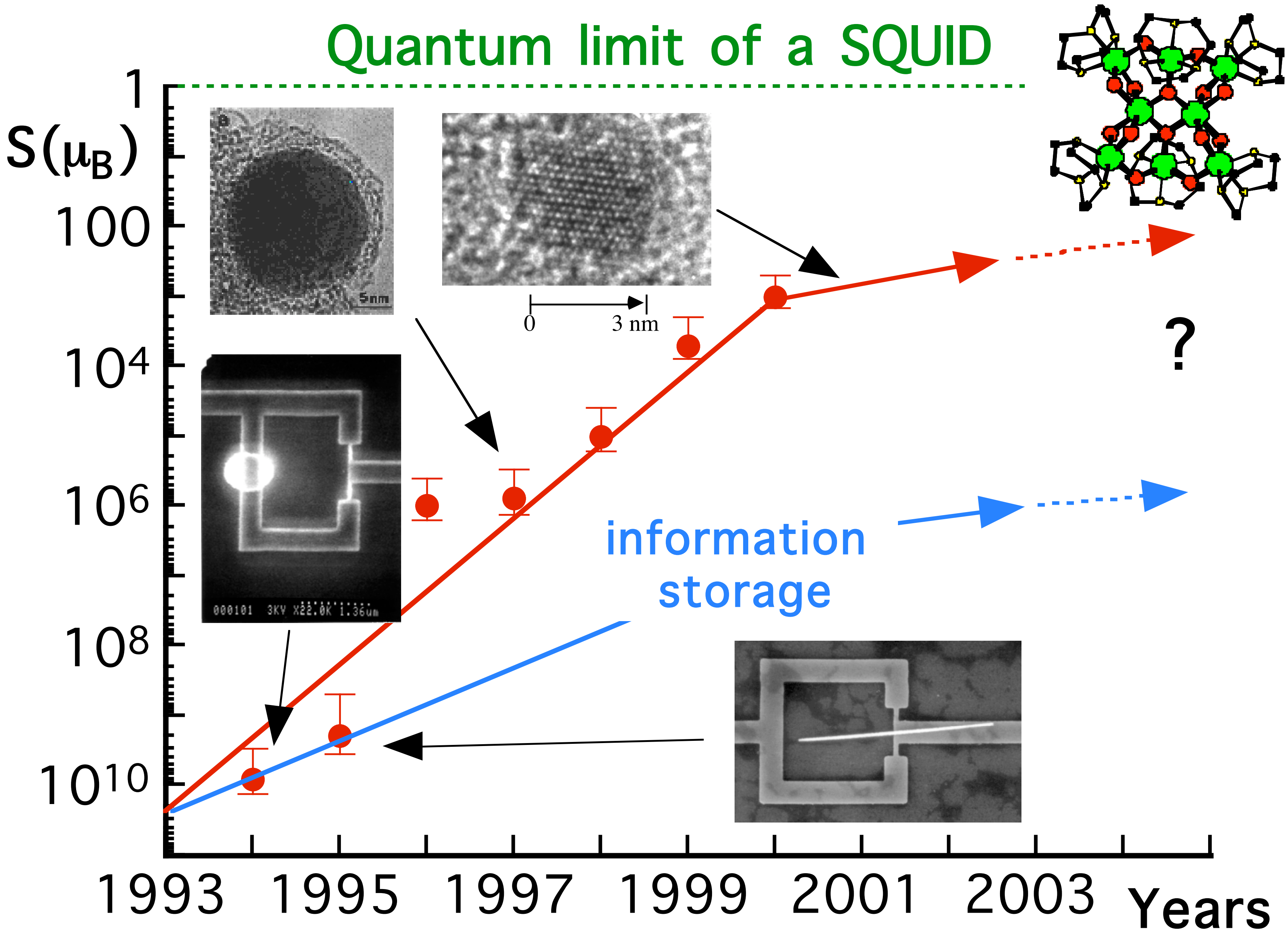

Towards molecular spintronics

ALEXANDRE R. ROCHA[1], VÍCTOR M. GARCÍA-SUÁREZ[2], STEVE W. BAILEY[3], COLIN J. LAMBERT[3], JAIME FERRER[2] AND STEFANO SANVITO[1]*

[1]Physics Department, Trinity College, Dublin 2, Ireland
[2]Departamento de Física, Facultad de Ciencias, Universidad de Oviedo, 33007 Oviedo, Spain
[3]Department of Physics, Lancaster University, Lancaster, UK
*e-mail: sanvitos@tcd.ie

nature materials | VOL 4 | APRIL 2005 | www.nature.com/naturematerials

The ability to manipulate electron spin in organic molecular materials offers a new and extremely tantalizing route towards spin electronics, both from fundamental and technological points of view. This is mainly due to the unquestionable advantage of weak spin–orbit and hyperfine interactions in organic molecules, which leads to the possibility of preserving spin-coherence over times and distances much longer than in conventional metals or semiconductors. Here we demonstrate theoretically that organic spin valves, obtained by sandwiching an organic molecule between magnetic contacts, can show a large bias-dependent magnetoresistance and that this can be engineered by an appropriate choice of molecules and anchoring groups. Our results, obtained through a combination of state-of-the-art non-equilibrium transport methods and density functional theory, show that although the magnitude of the effect varies with the details of the molecule, large magnetoresistance can be found both in the tunnelling and the metallic limit.

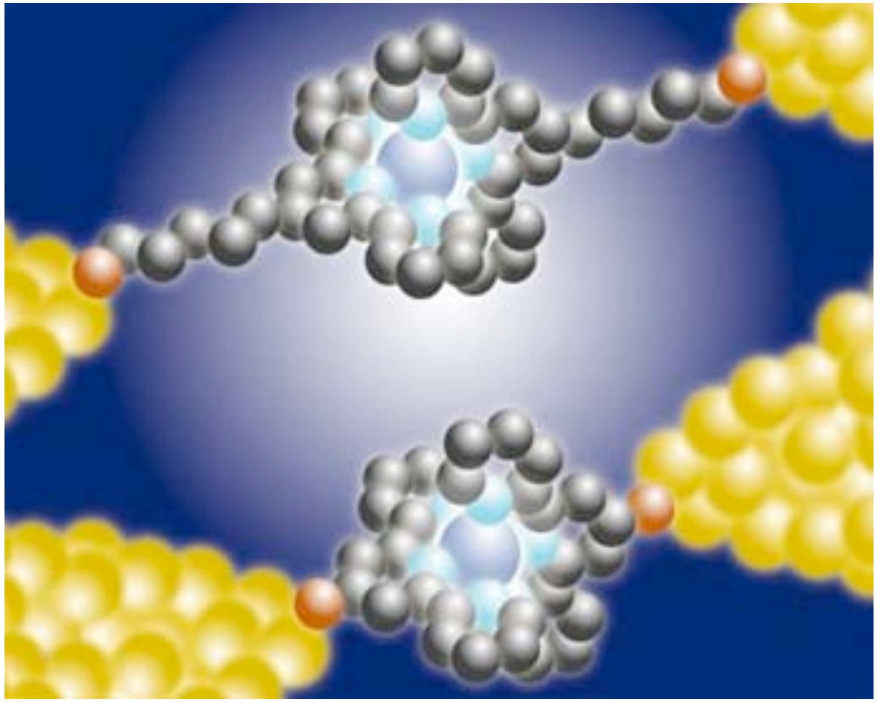

MCEUEN group (Cornell)

Molecular spintronics

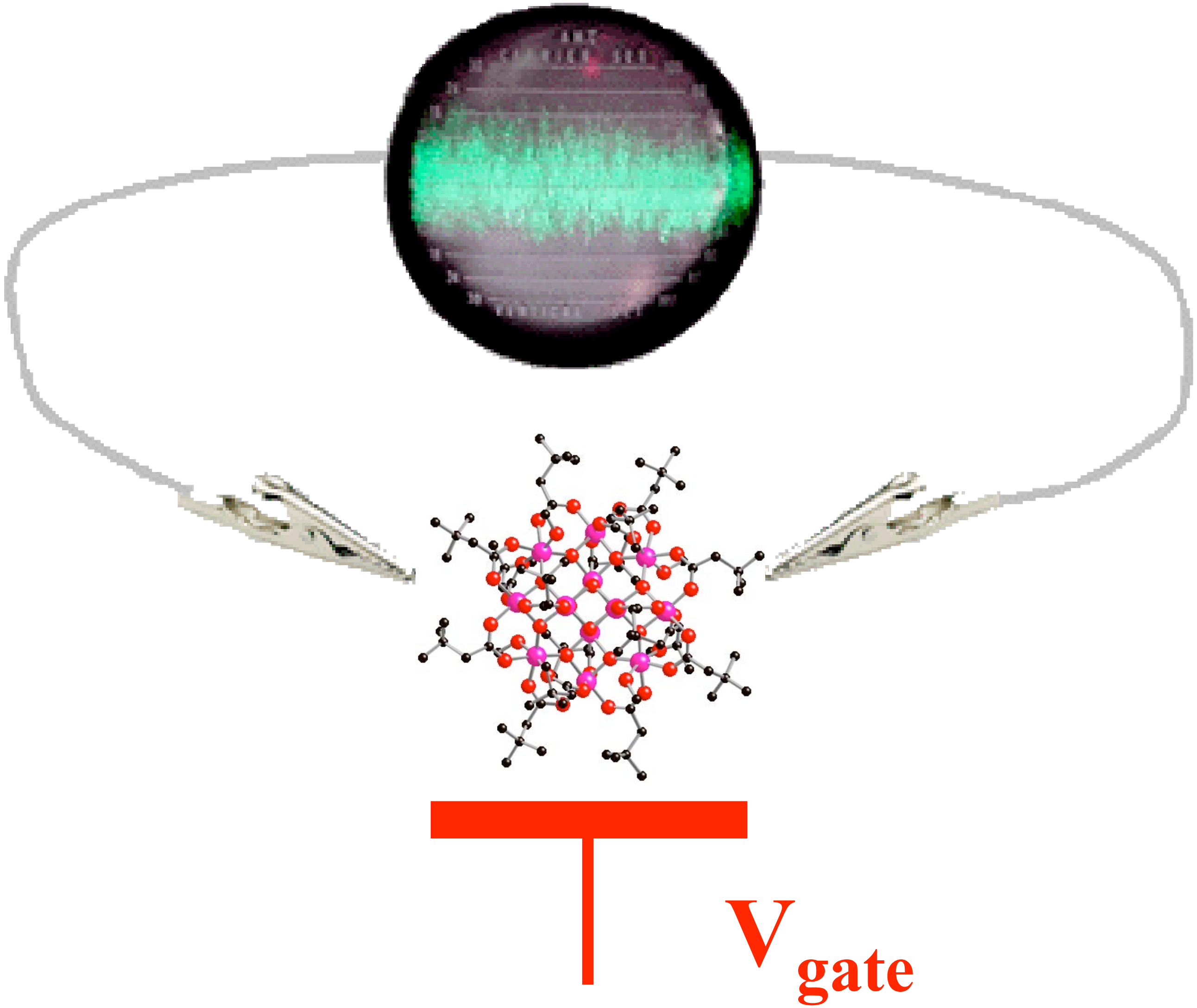

Molecular spintronics : first devices ..

Molecular transistor :

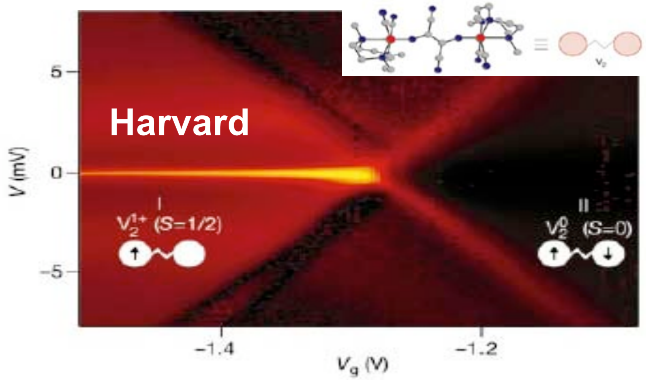

Liang et al., Nature ***417****, 2002.*

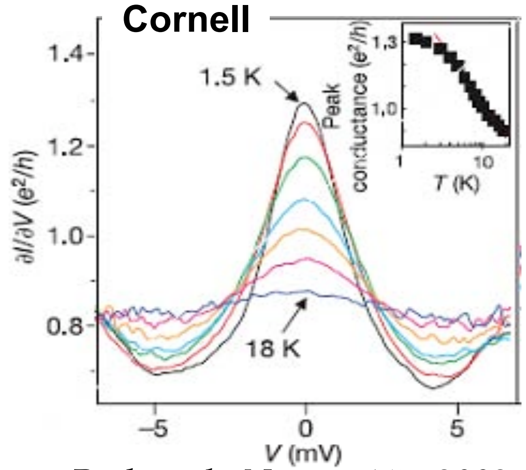

Park et al., Nature ***417****, 2002.*

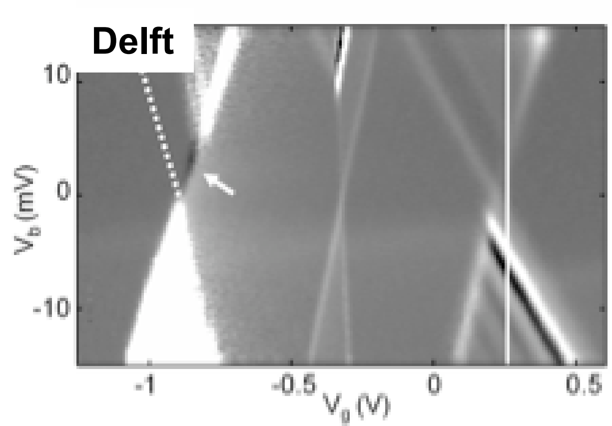

H. Heersche et al., PRL **96**, 206801 (2006)

Ferromagnetic electrodes :

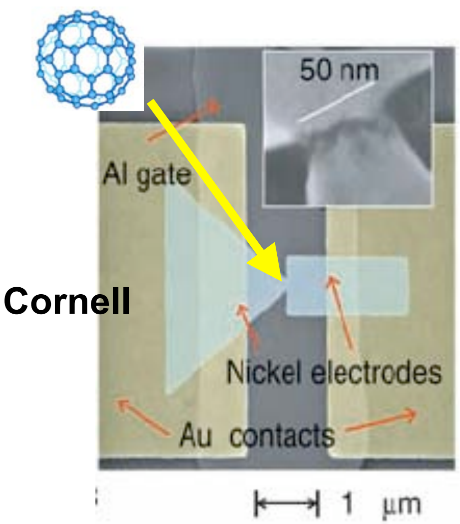

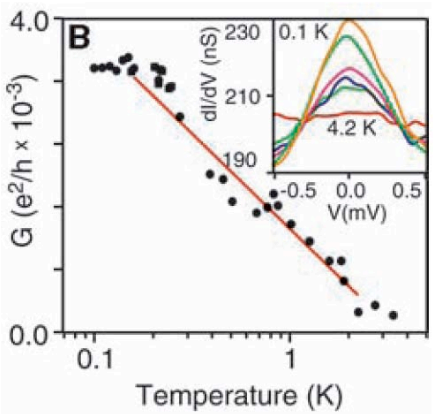

Pasupathy et al., Science ***306****, 2004.*

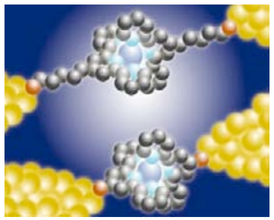

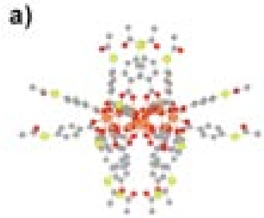

Harvard, Cornell, Berkeley, …

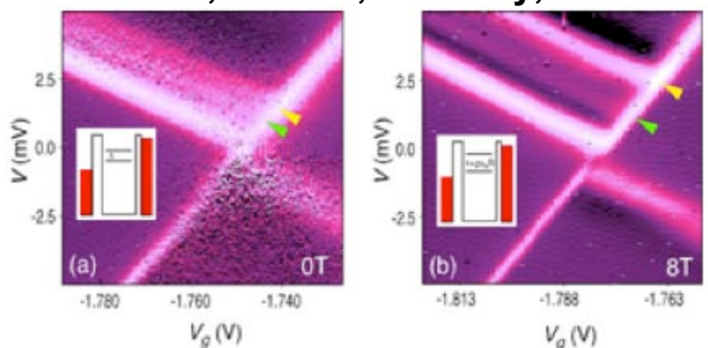

M.-H. Jo et al., Nano Lett., 6, 2014 (2006)

Molecular spintronics

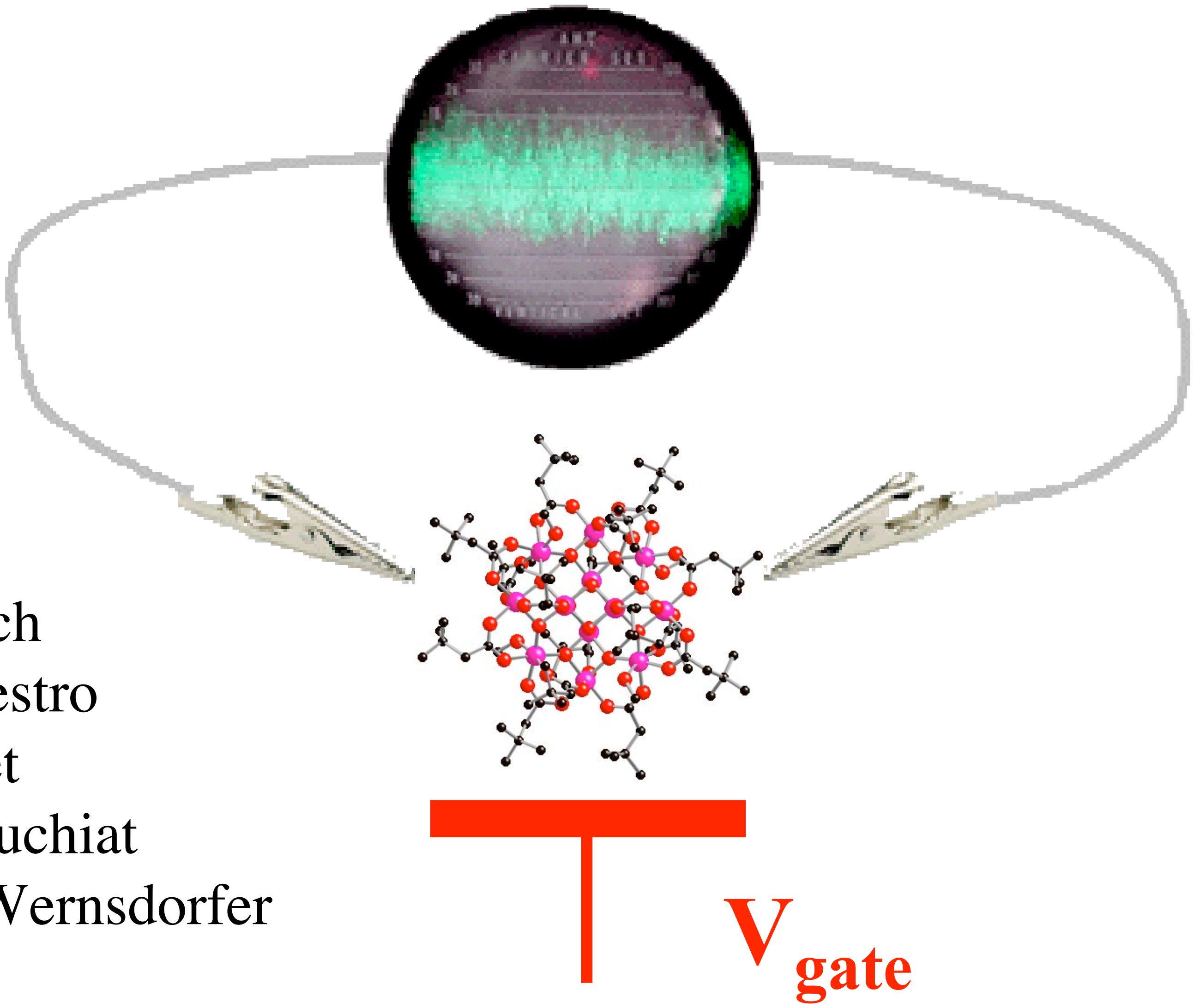

Nicolas Roch
Franck Balestro
Edgar Bonet
Vincent Bouchiat
Wolfgang Wernsdorfer

Electromigration

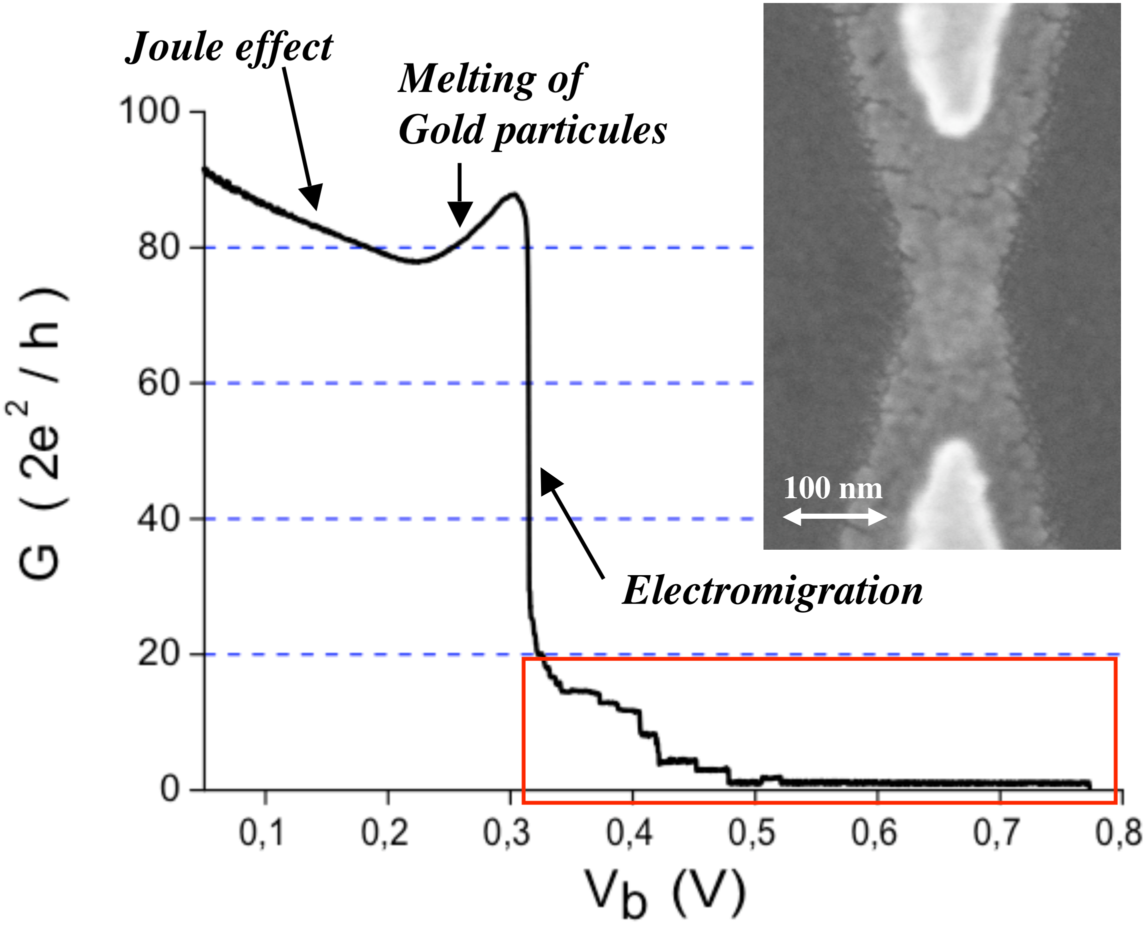

Local temperature ≈ 500K

M. F. Lambert and *al.*, NanoTechnology, **14**, 772, 2003
T. Taychatanapat, and *al.*, Nano Lett., **7**, 652, 2007

Electromigration depends on

- ***Material used (Gold, Alu, …)***
- ***Cooling power***
- ***Serie's resistor***
- ***Junction resistor***
- ***Ramping rate (10mV/s)***
- ***Feedback loop (1µs)***

Conductance steps in Gold junction

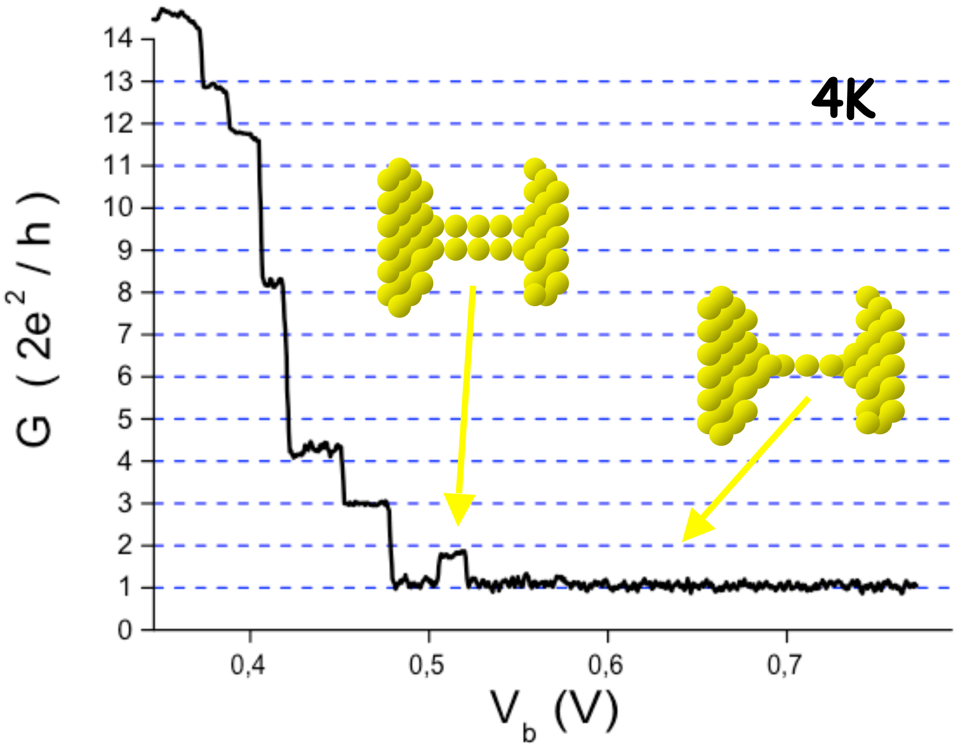

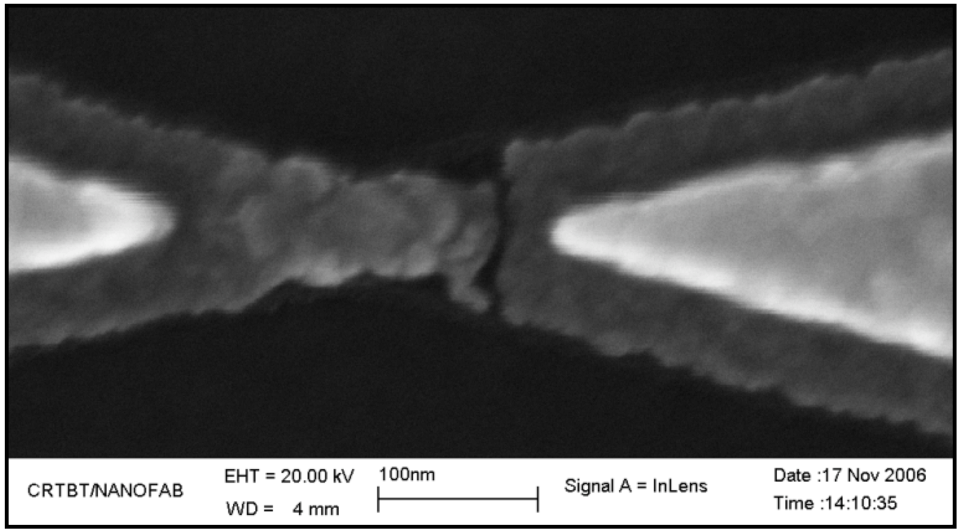

Molecular spintronics

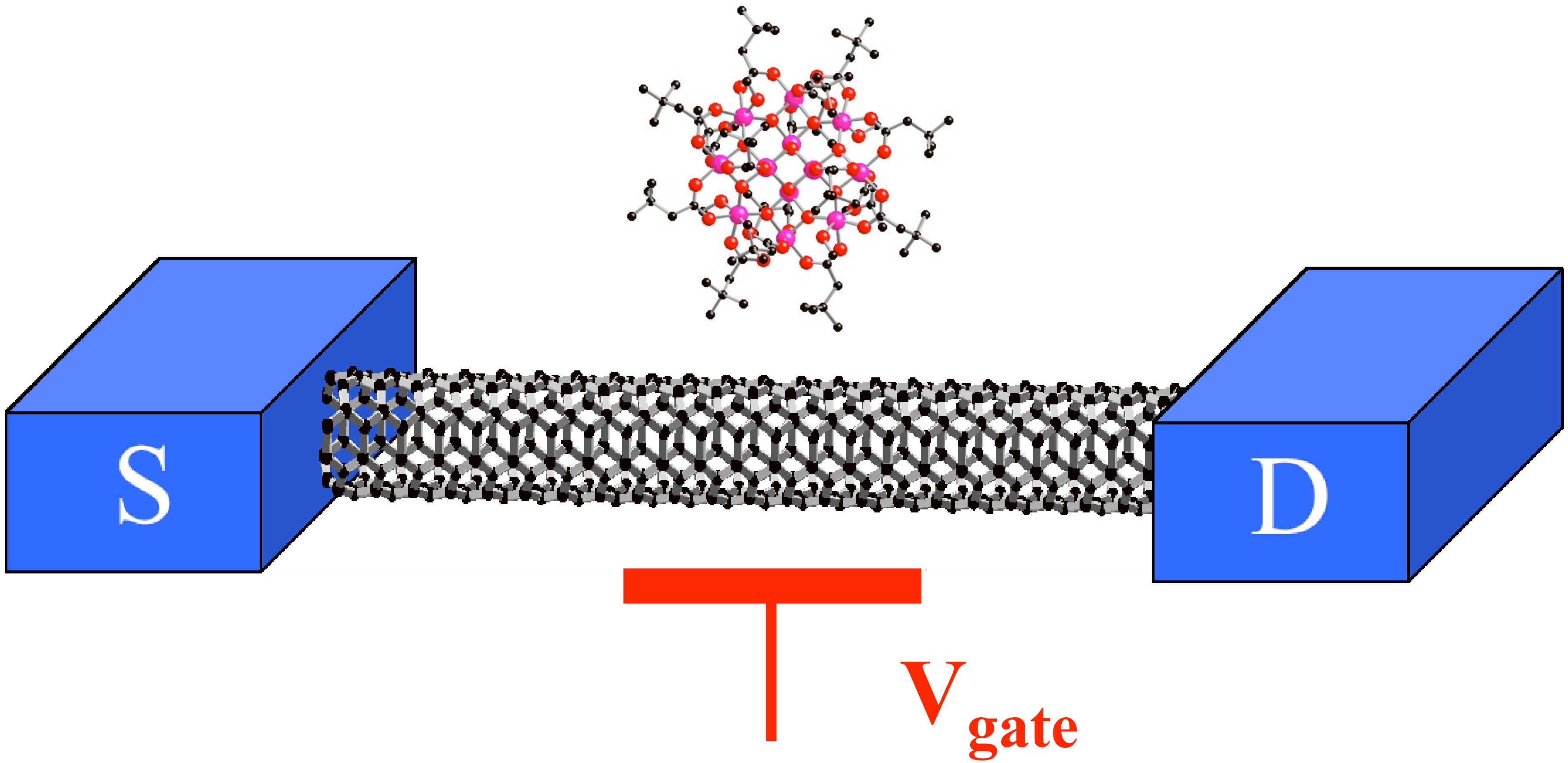

Molecular spintronics

Cecile Delacour
Clemens Winkelmann
Lapo Bogani
Laetitia Marty
Romain Maurand
Vincent Bouchiat
Wolfgang Wernsdorfer

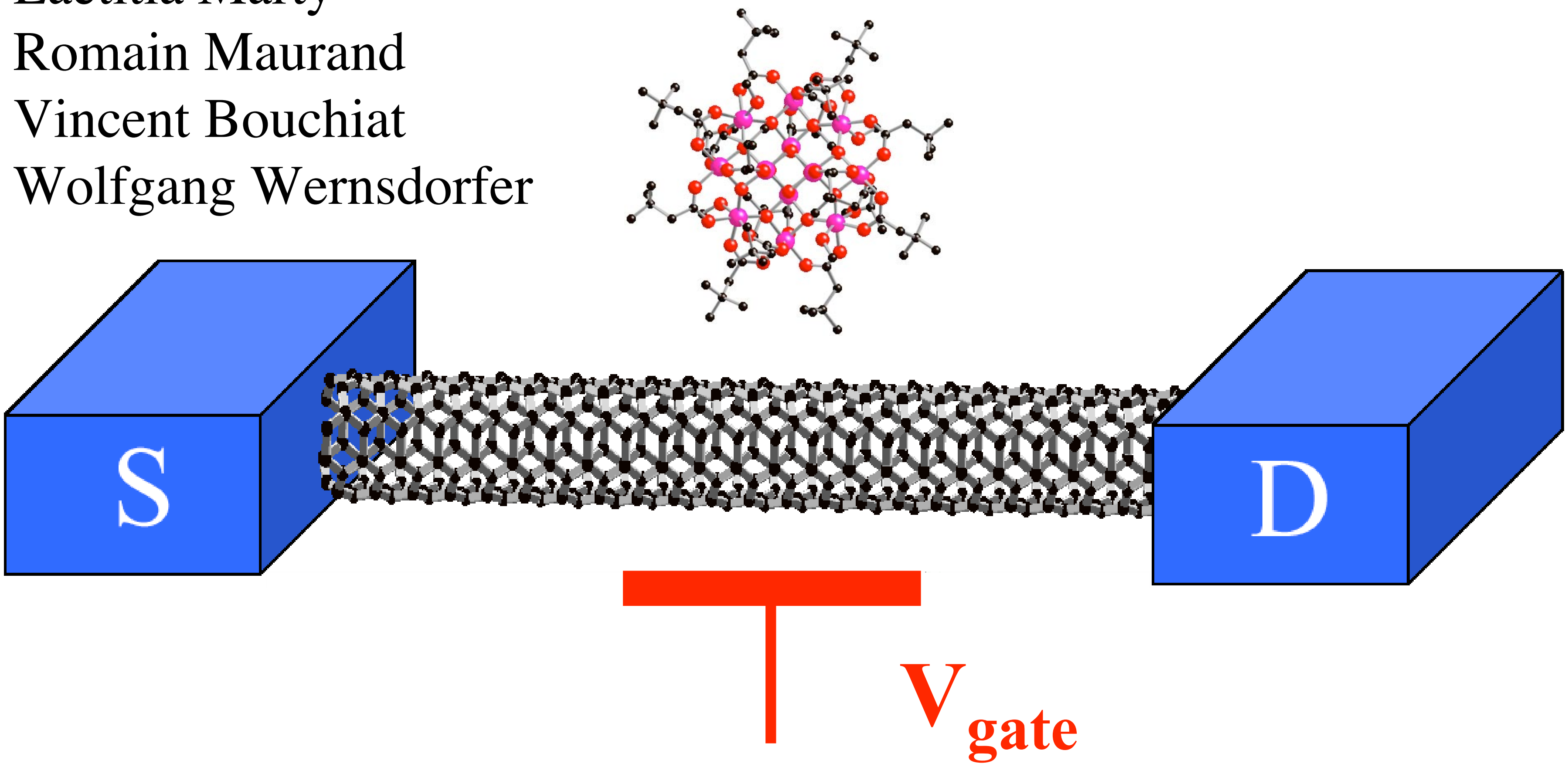

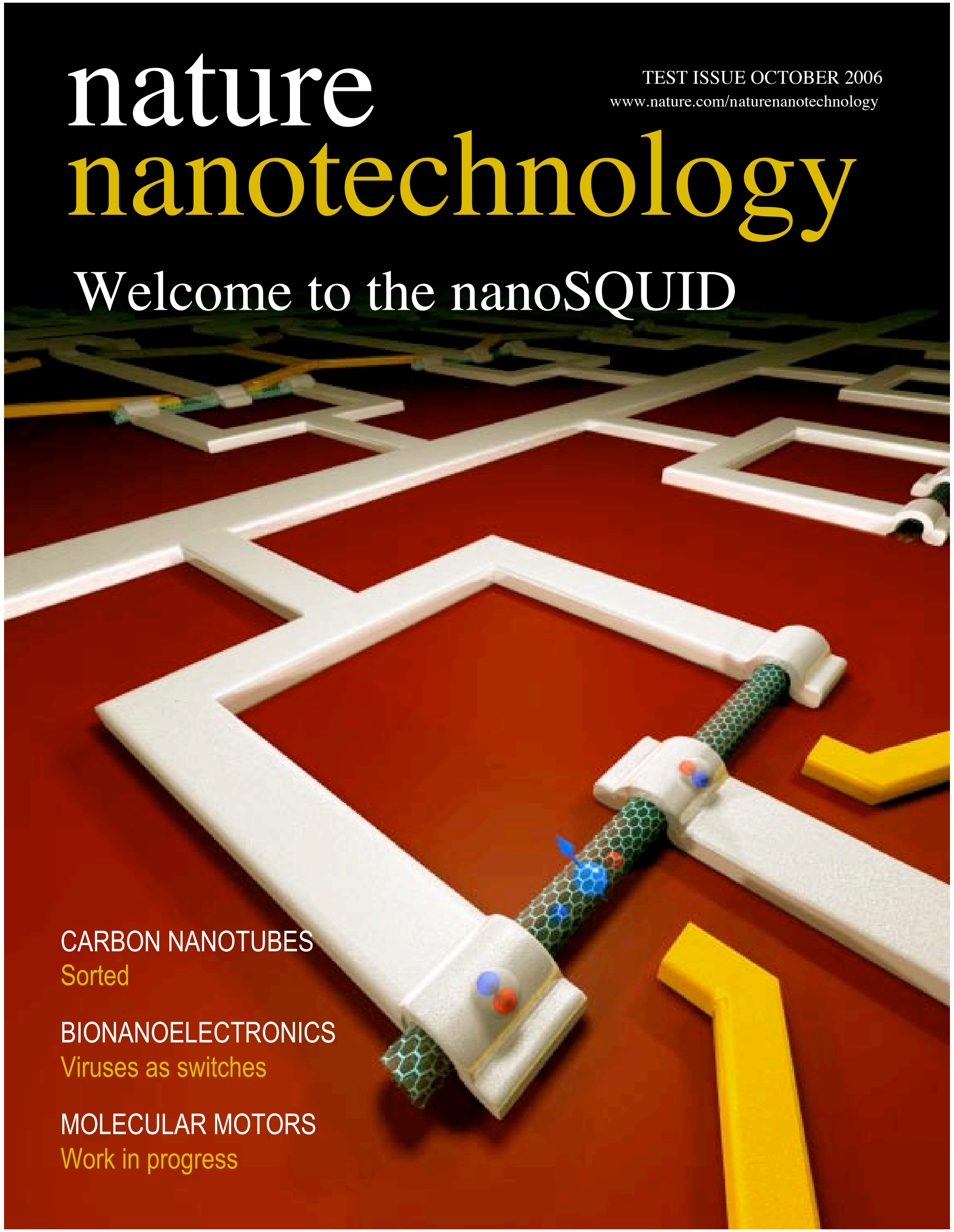

**J.-P. Cleuziou,
W. Wernsdorfer,
V. Bouchiat,
Th. Ondarçuhu,
M. Monthioux**

**Nature
Nanotechnology,
1, 53 (2006)**

Magnetization switching of single molecules

micro-SQUID versus nano-SQUID (CNT-SQUID)

Optimising the flux coupling factor for small samples

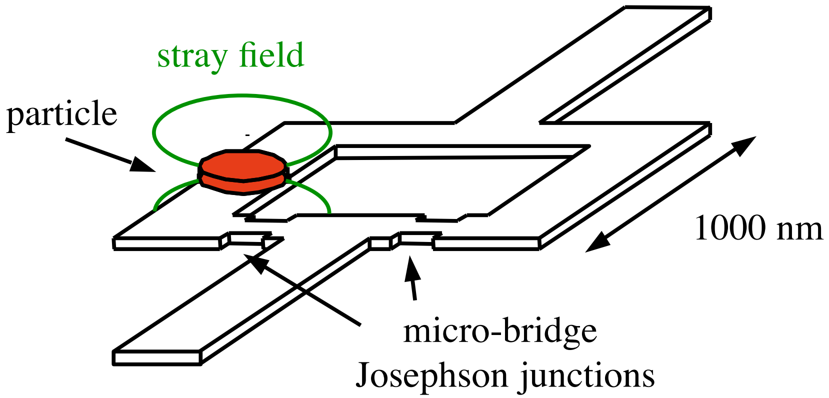

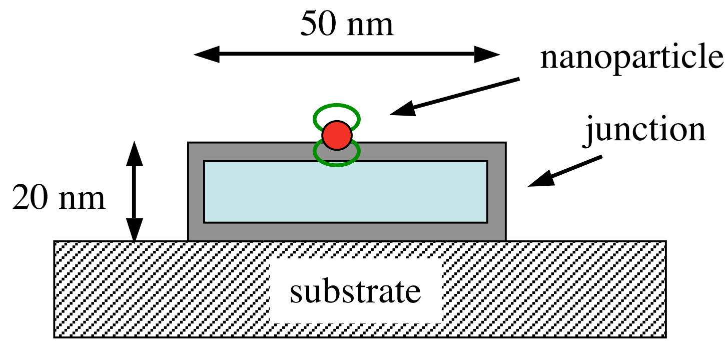

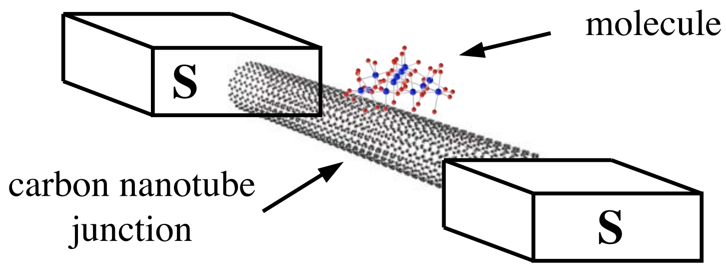

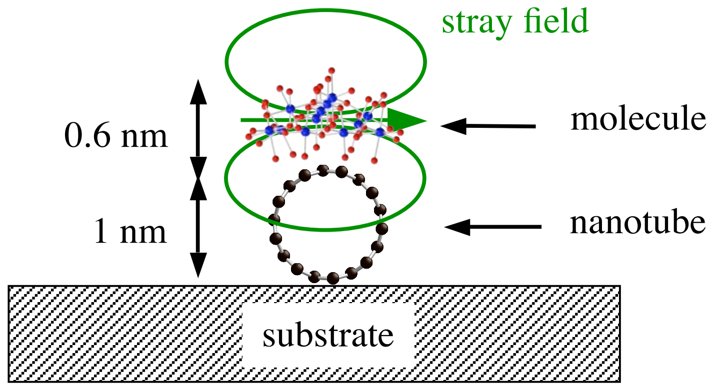

Carbon nanotube SQUID fabrication

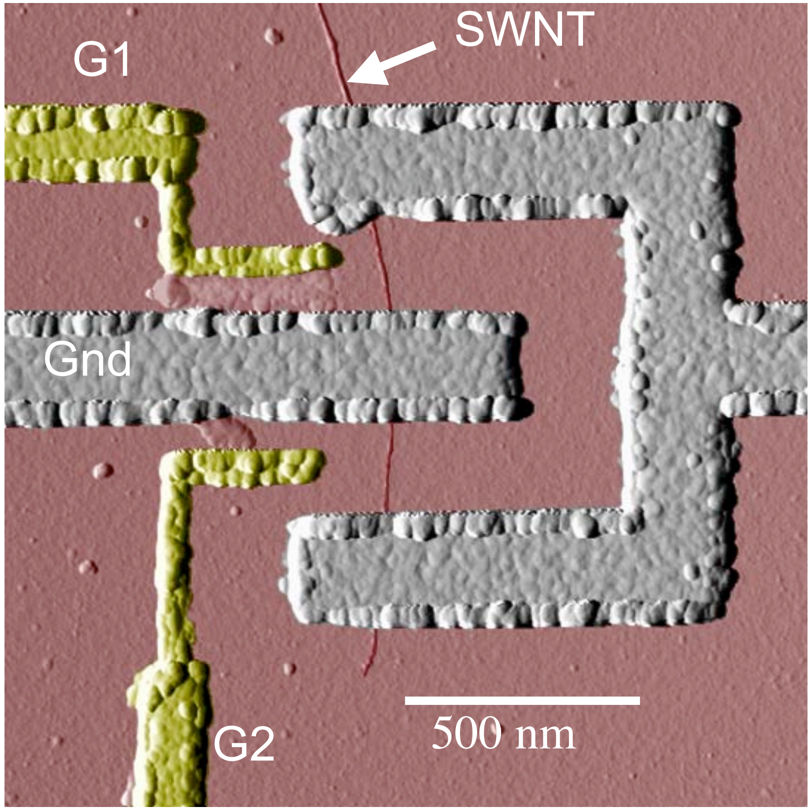

- single-walled CNTs: Rice University.
- dispersed in water by sonication using sodium dodecyl sulphate (SDS) surfactant.
- n-doped silicon substrate with 350 nm thick thermally grown SiO_2 => backgate
- functionalized => monolayer of aminopropyltriethoxysilane
- substrate was dipped in the dispersion of CNTs and withdrawn (combing technique)
- thoroughly washed in distilled water
- nanotube location with AFM
- aligned e-beam lithography
- metal electrodes: 3 nm Pd + 50 nm Al
- R ≈ 30 kΩ and no significant gate effect at 300 K
- fabricated about 100 CNT-SQUIDs and 300 CNT-superconducting transistors using single-walled CNTs, ropes of CNTs, and multi-walled CNTs: ≈ 30 % worked

J.-P. Cleuziou, *CEMES-CNRS, Toulouse, France*
F. Carcenac, *RTB-LAAS, Toulouse, France*

Combing technique

• substrate was dipped in the dispersion of CNTs and withdrawn

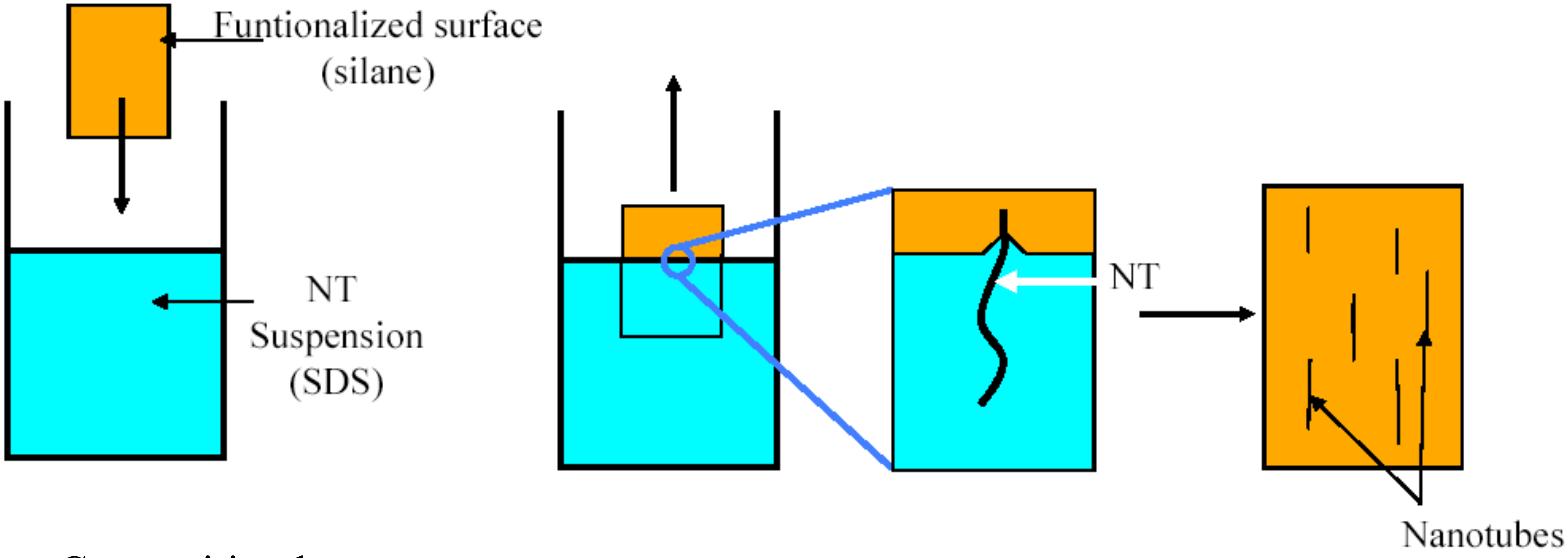

Competition between:

⇒ Nanotube adsorption on silanized surface

⇒ Capillary → alignment

S. Gerdes, T. Ondarcuhu, S. Cholet, C. Joachim,
Europhys. Lett. **48,** 292 (1999).

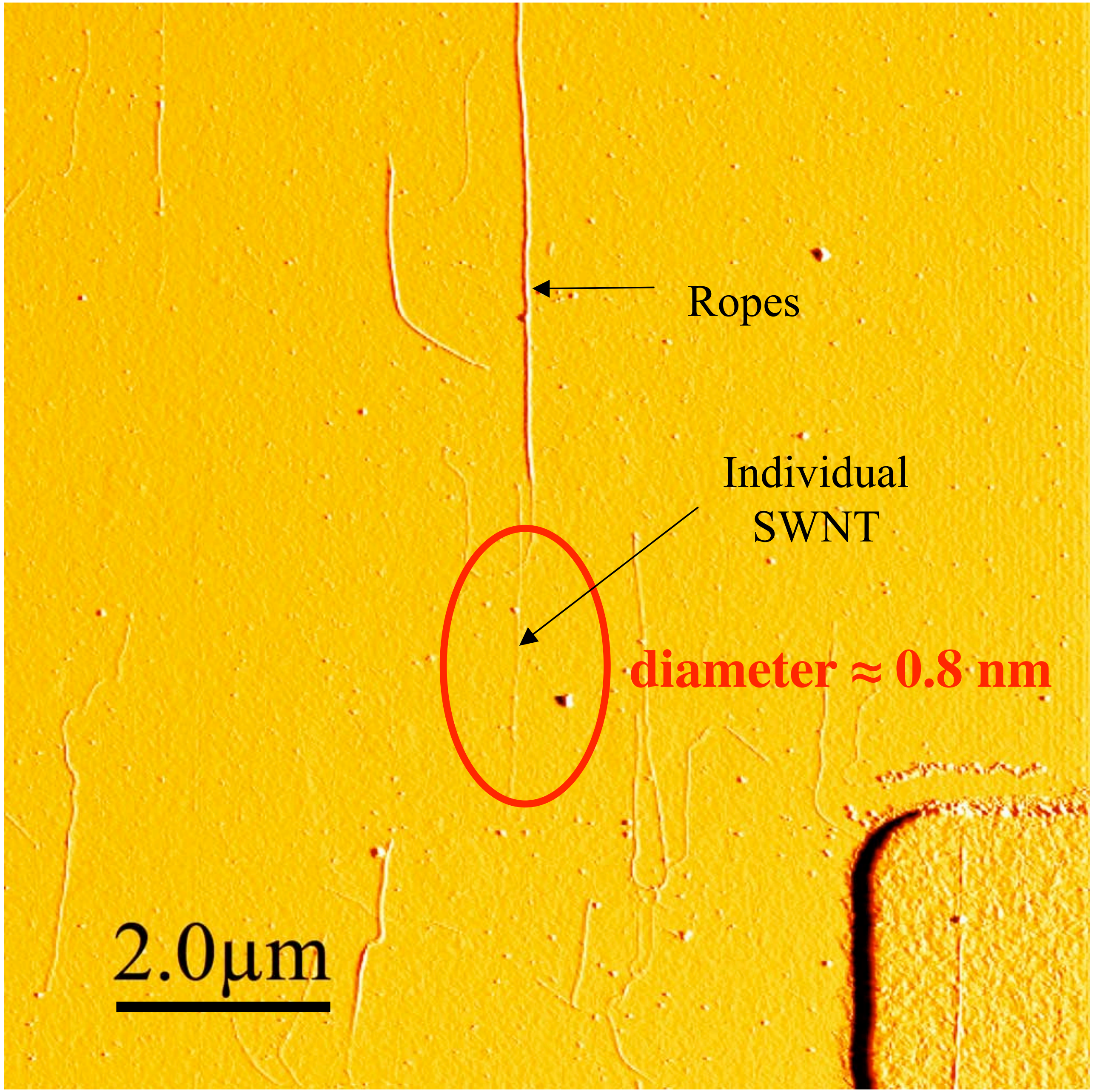

CNT deposition

Combing technique

S. Gerdes,
T. Ondarcuhu,
S. Cholet,
C. Joachim,
Europhys. Lett.
48, 292 (1999).

E-beam lithography

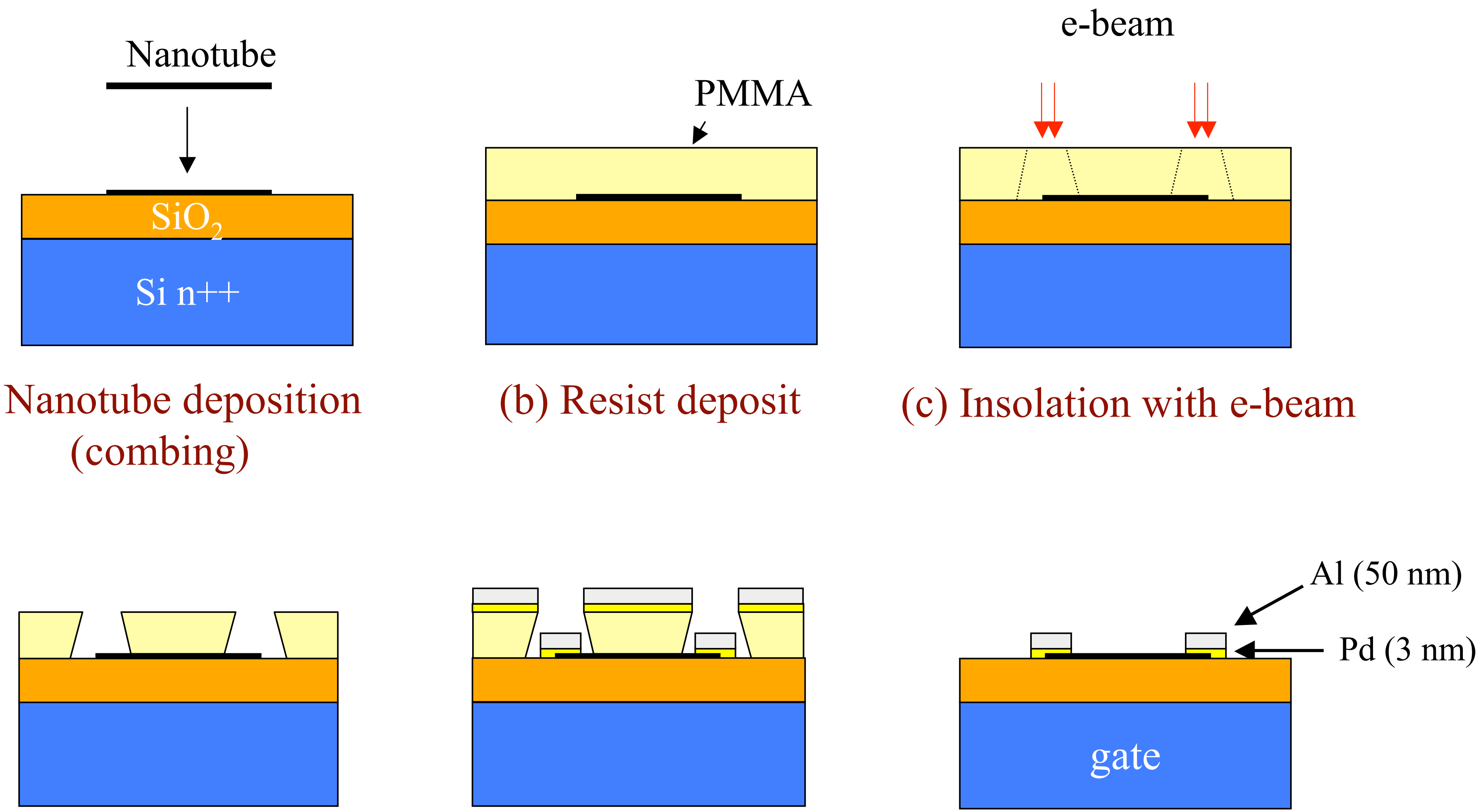

(a) Nanotube deposition (combing)

(b) Resist deposit

(c) Insolation with e-beam

(d) Development

(e) Metal evaporation

(f) Lift-off

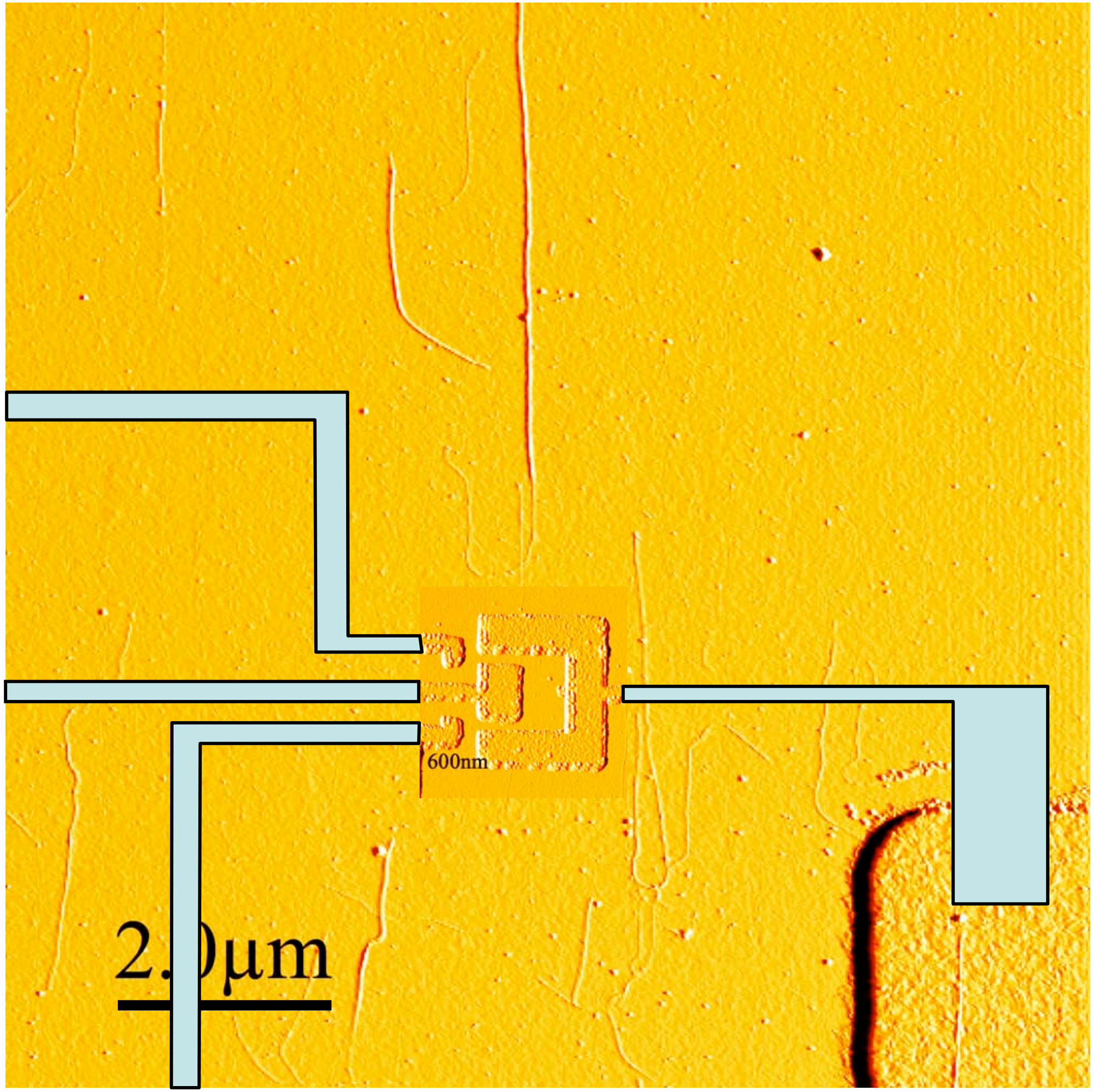

Aligned e-beam lithography

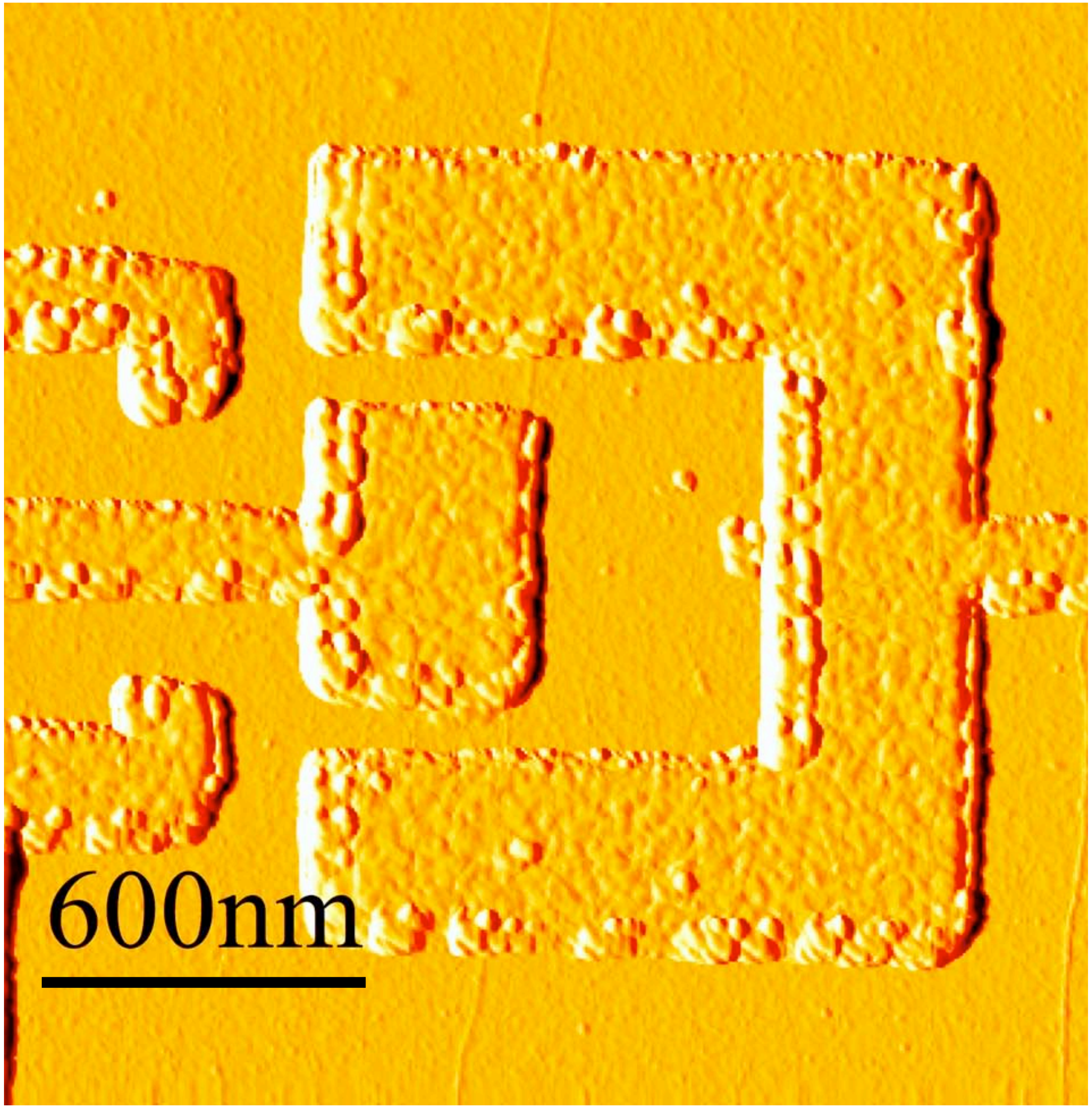

CNT-SQUID
or
nanoSQUID

SWNT junction

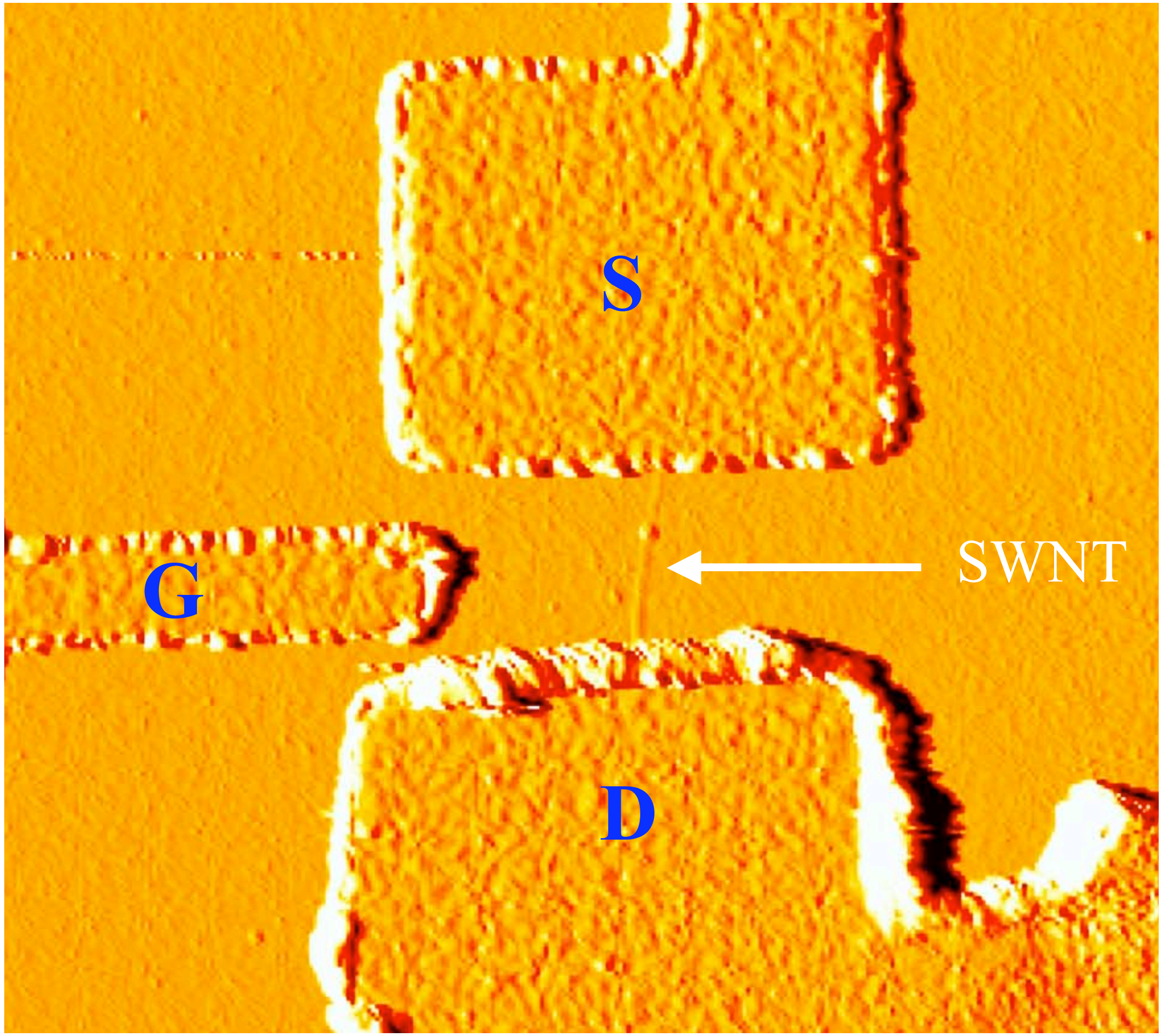

Superconducting transistor

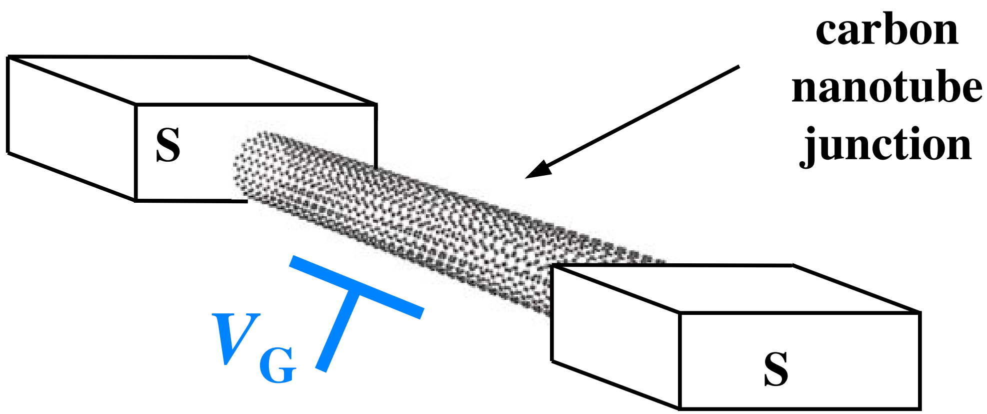

Energy level schematics

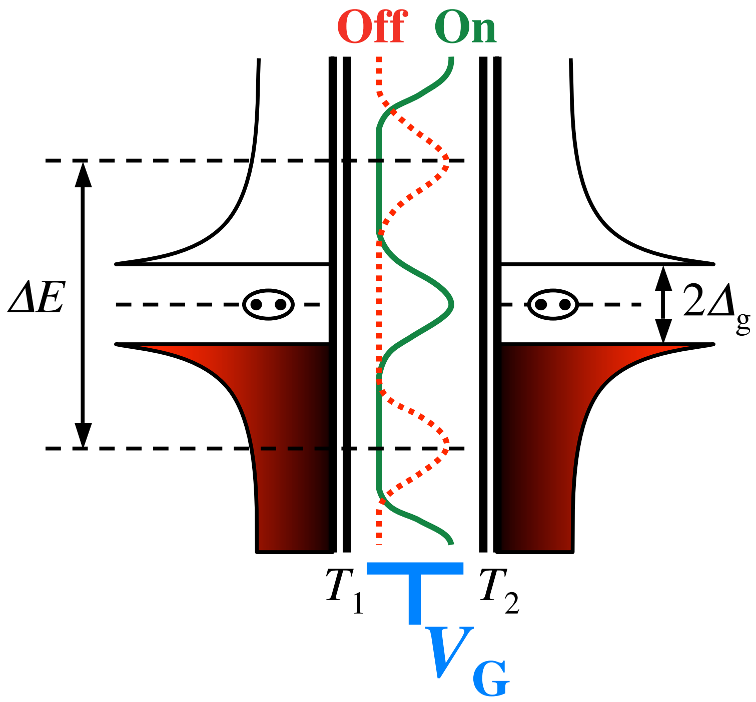

P. Jarillo-Herrero, et al., *Nature* **439**, 953-956 (2006).
H.I. Jørgensen et al. PRL 96, 207003 (2006).
J.-P. Cleuziou et al., unpublished (2006).
etc.

Electronic transport through a quantum dot (Charging effects)

Three categories depending on the ratio of

dot coupling to the leads: $h\Gamma$ ⟺ charging energy: U

i) $h\Gamma << U$ (Closed QD regime): Charging effects dominate transport (Coulomb blockade)

ii) $h\Gamma <= U$ (Intermediate transparency regime): Charging effects important, but higher-order tunneling processes significant too (cotunneling and Kondo effect).

iii) $h\Gamma >> U$ (Open QD regime): Quantum interference (Fabry-Perot)

Electronic transport properties and Kondo effect of CNT junctions

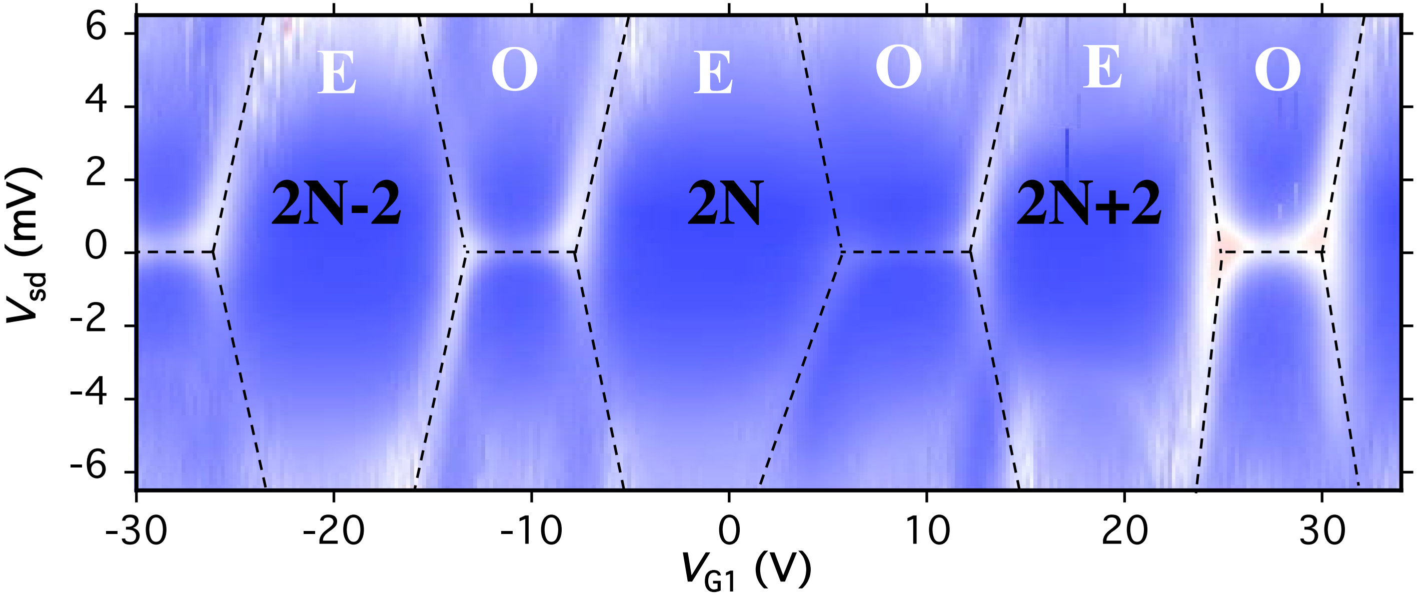

35 mK

H_z **= 50 mT**

Superconductivity of the leads is supressed

Conductance ***dI/dV***

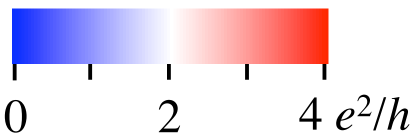

U_c/e = 6 meV

$\delta E/e$ = 9 meV

Γ = 1 meV

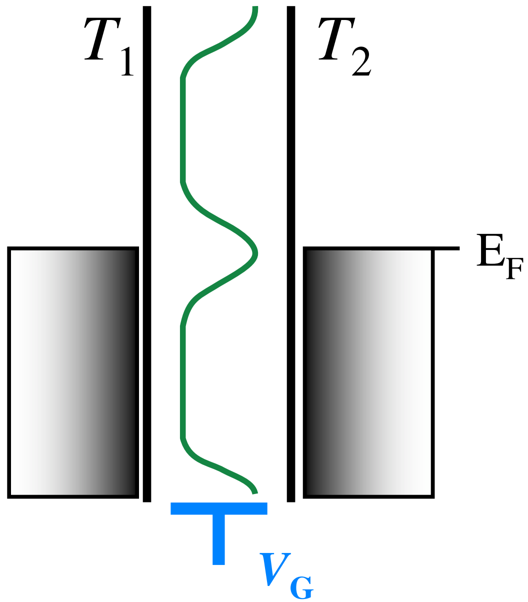

$\delta E = hv_F/2L$

v_F = 8.1 x 10^5 m/s Fermi velocity in the CNT

$\Rightarrow$ L = 186 nm, comparable to CNT length of ≈ 200 nm

Kondo effect versus superconductivity

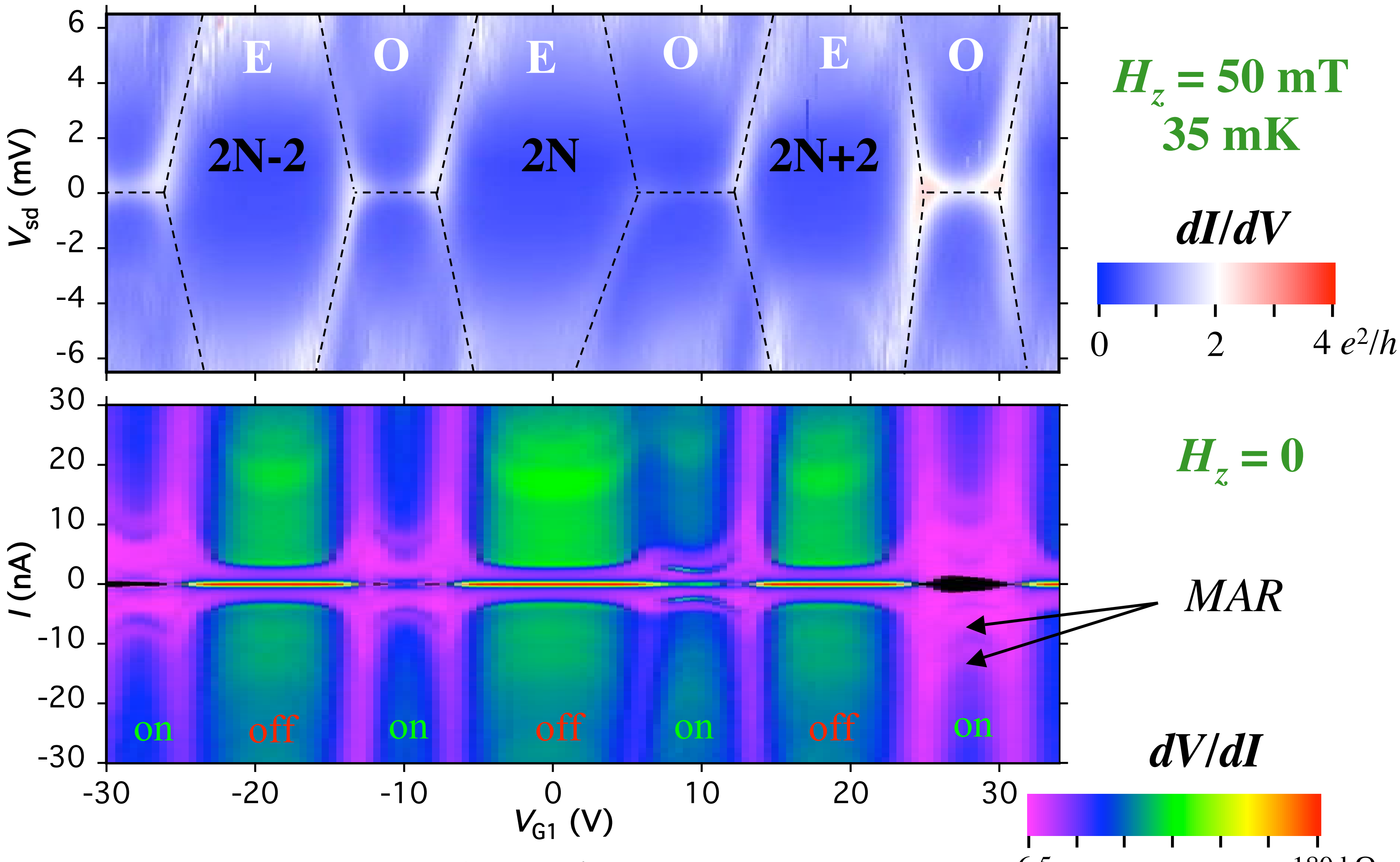

(see group of C. Schönenberger, 2002-04)

Gate voltage dependence of the switching current

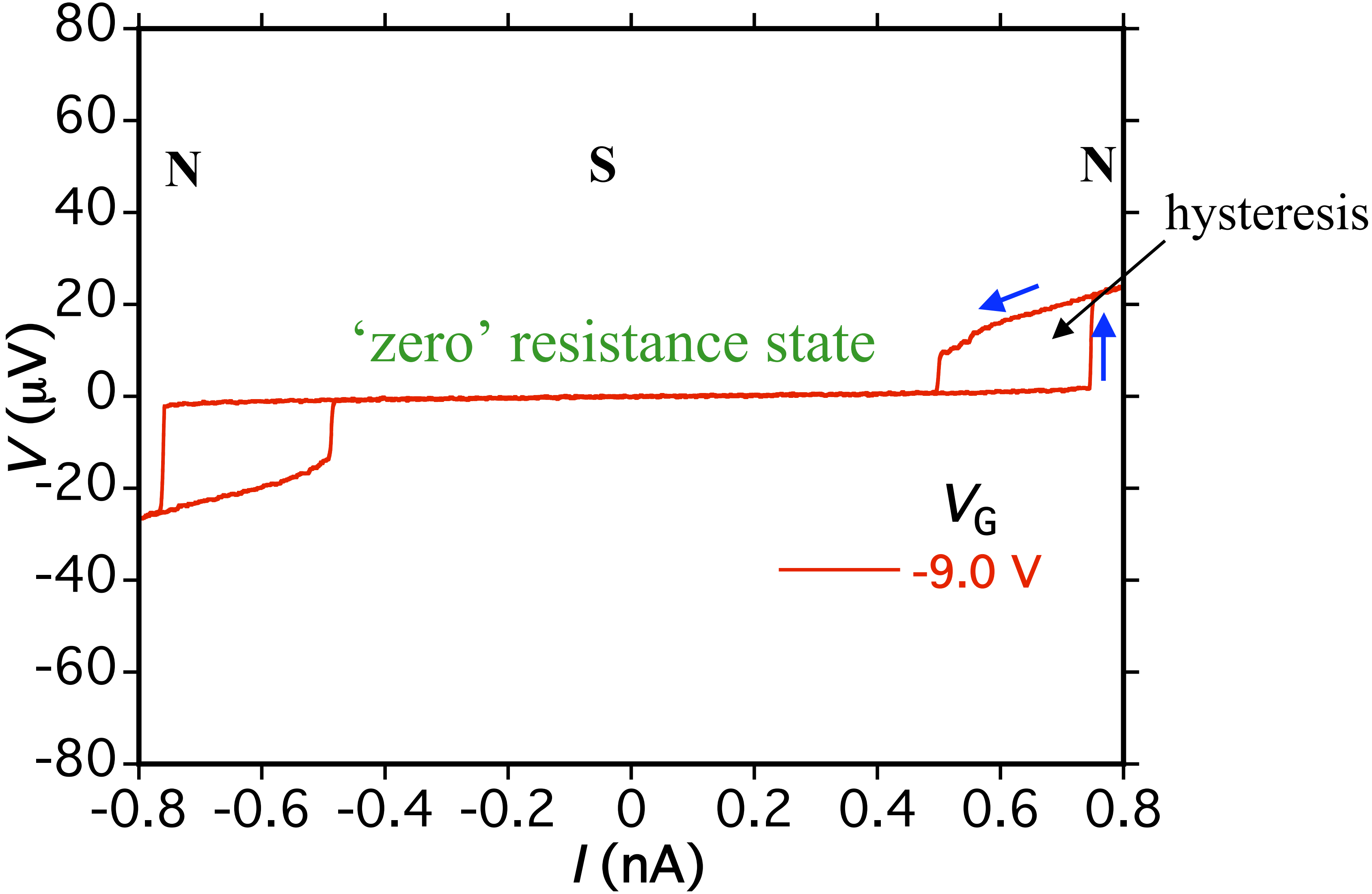

Gate voltage dependence of the switching current

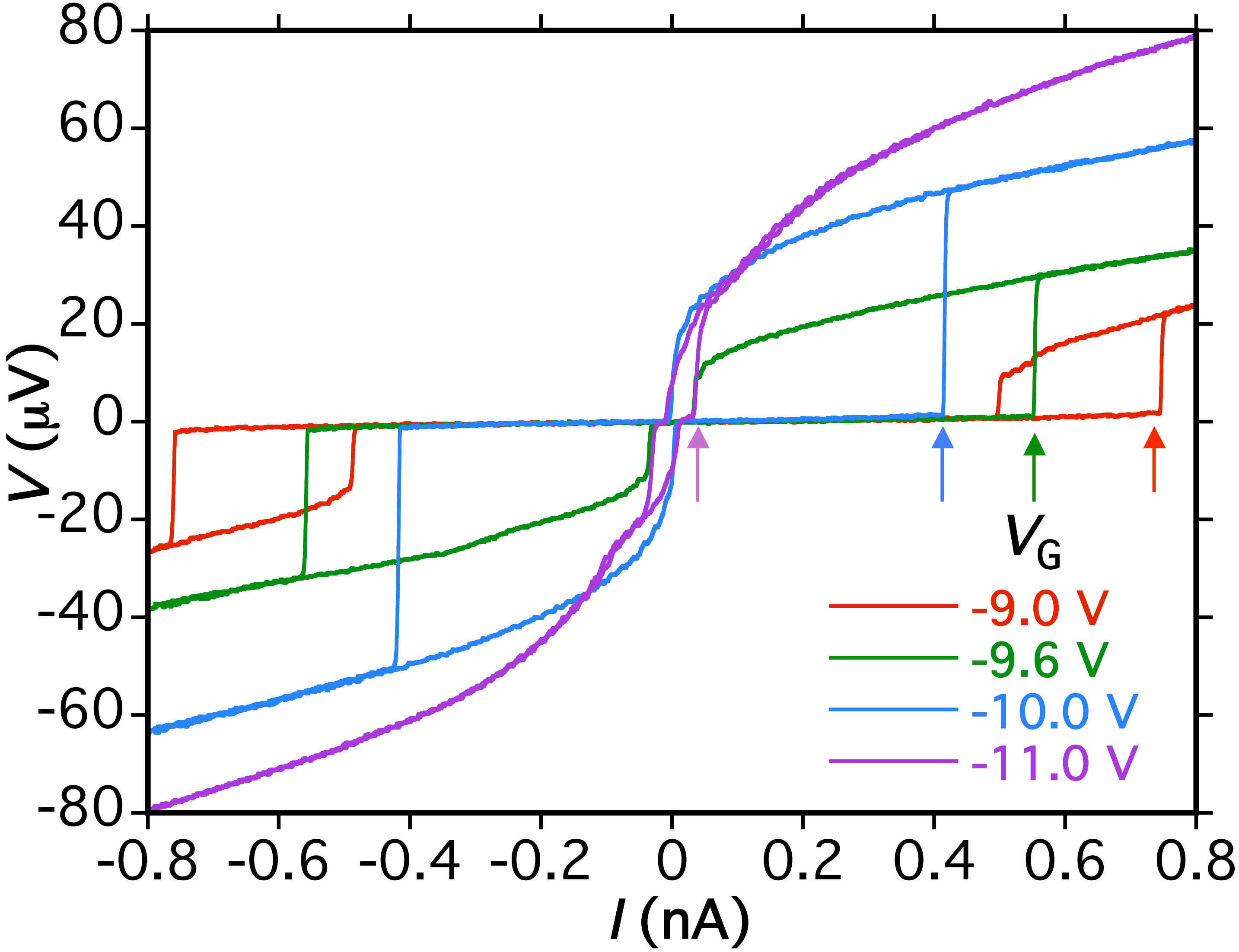

Tuning the dot coupling with the Pd thickness

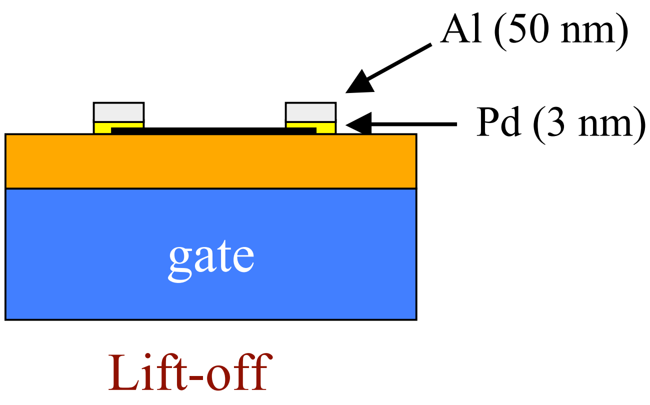

i) $h\Gamma << U$ (Closed QD regime): Pd < 4 nm

ii) $h\Gamma <= U$ (Intermediate transparency regime): 4 nm < Pd < 6 nm

iii) $h\Gamma >> U$ (Open QD regime): Pd > 7 nm

$h\Gamma \ll U$ (Closed QD regime): Pd < 3 nm

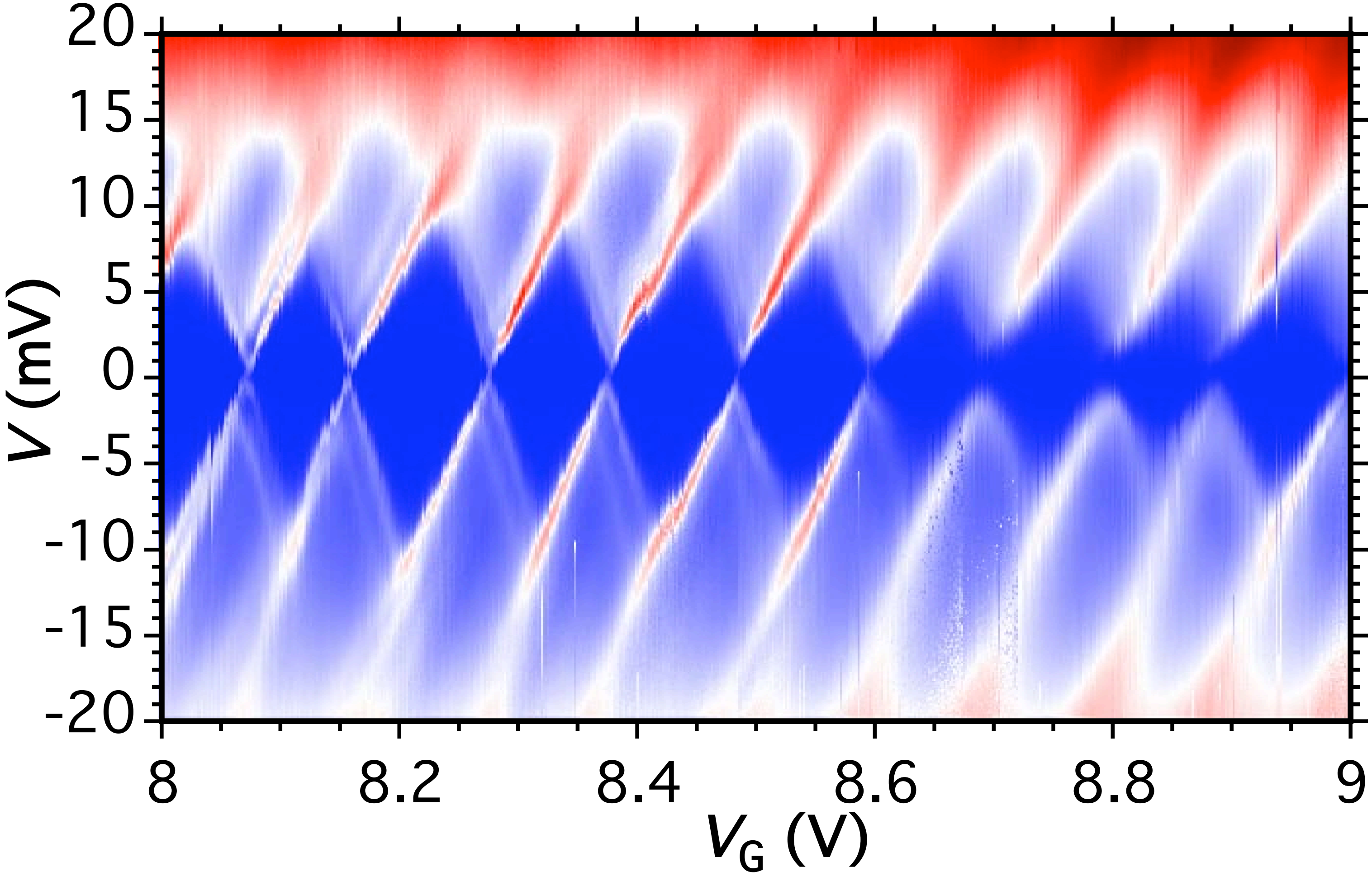

$h\Gamma$ <= U (Intermediate transparency regime): Pd – 4 nm

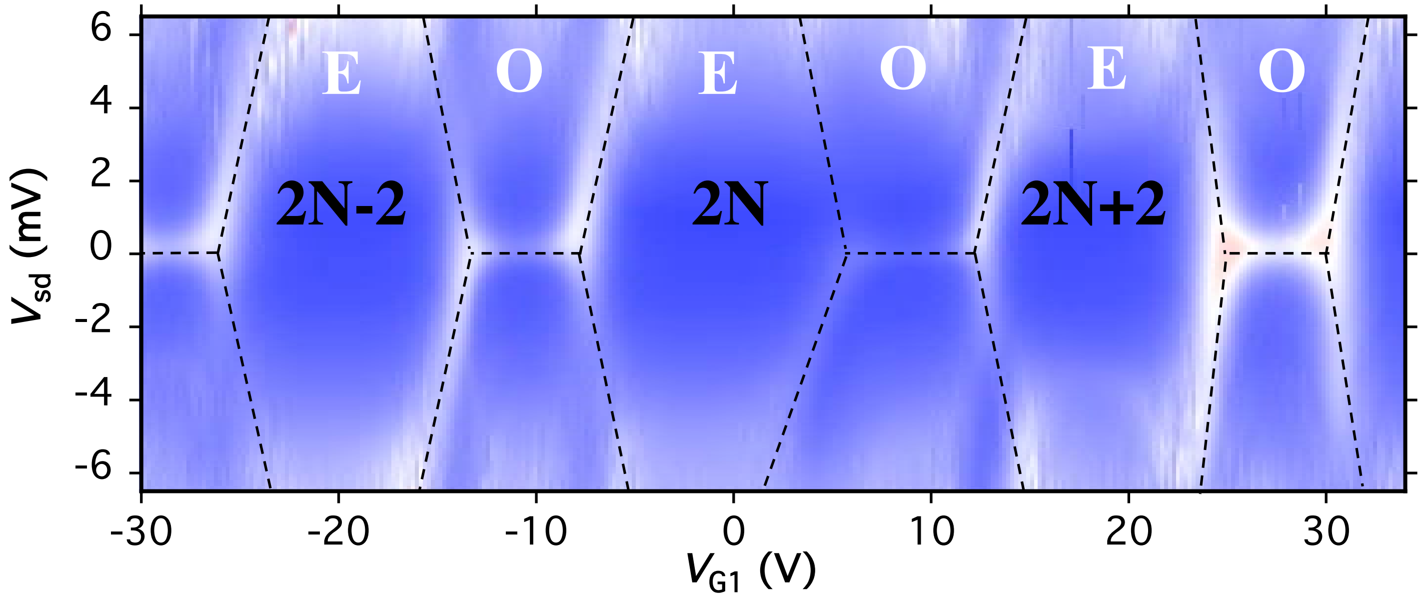

35 mK

H_z = 50 mT

Superconductivity of the leads is supressed

Conductance *dI/dV*

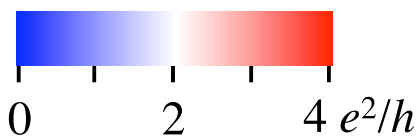

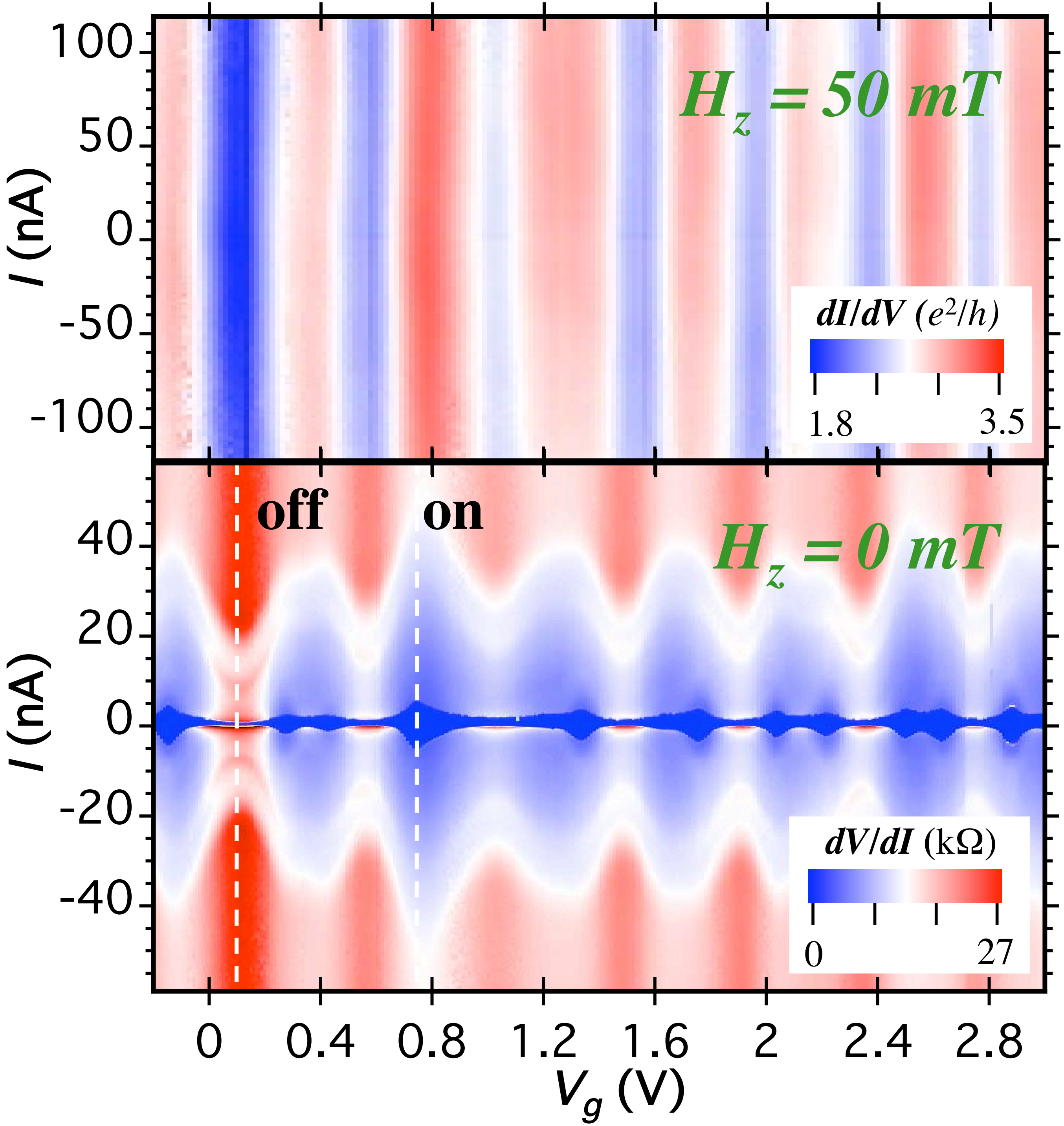

Electronic transport properties of CNT junctions

hΓ >> U

Open QD regime

Pd – 7 nm

Backgate and sidegate

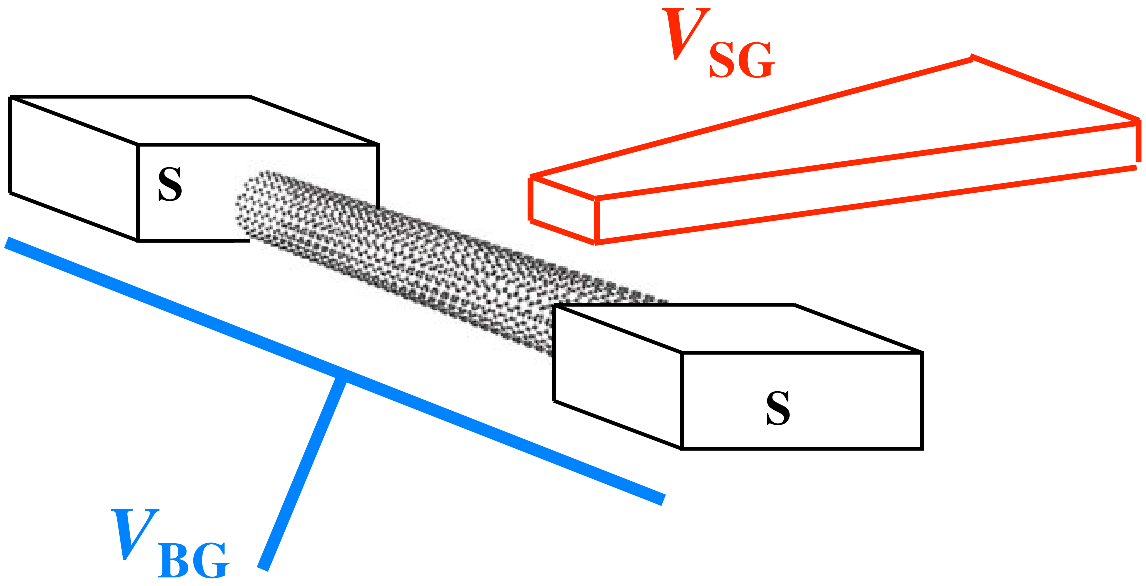

cond-mat/0610622

Tuning the Kondo effect with back and side gates - Application to carbon nanotube superconducting quantum interference devices and pi-junctions
J.-P. Cleuziou, W. Wernsdorfer, V. Bouchiat, Th. Ondarcuhu, M. Monthioux

Backgate versus sidegate

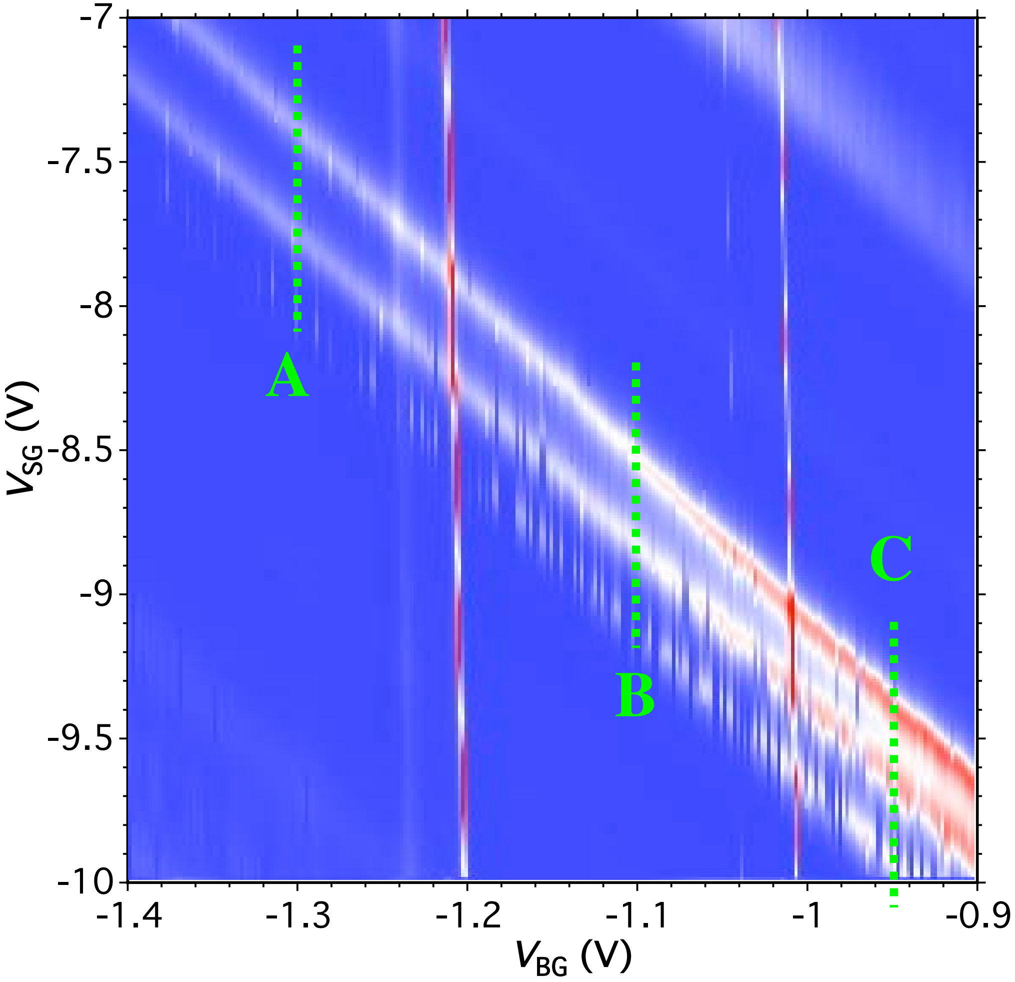

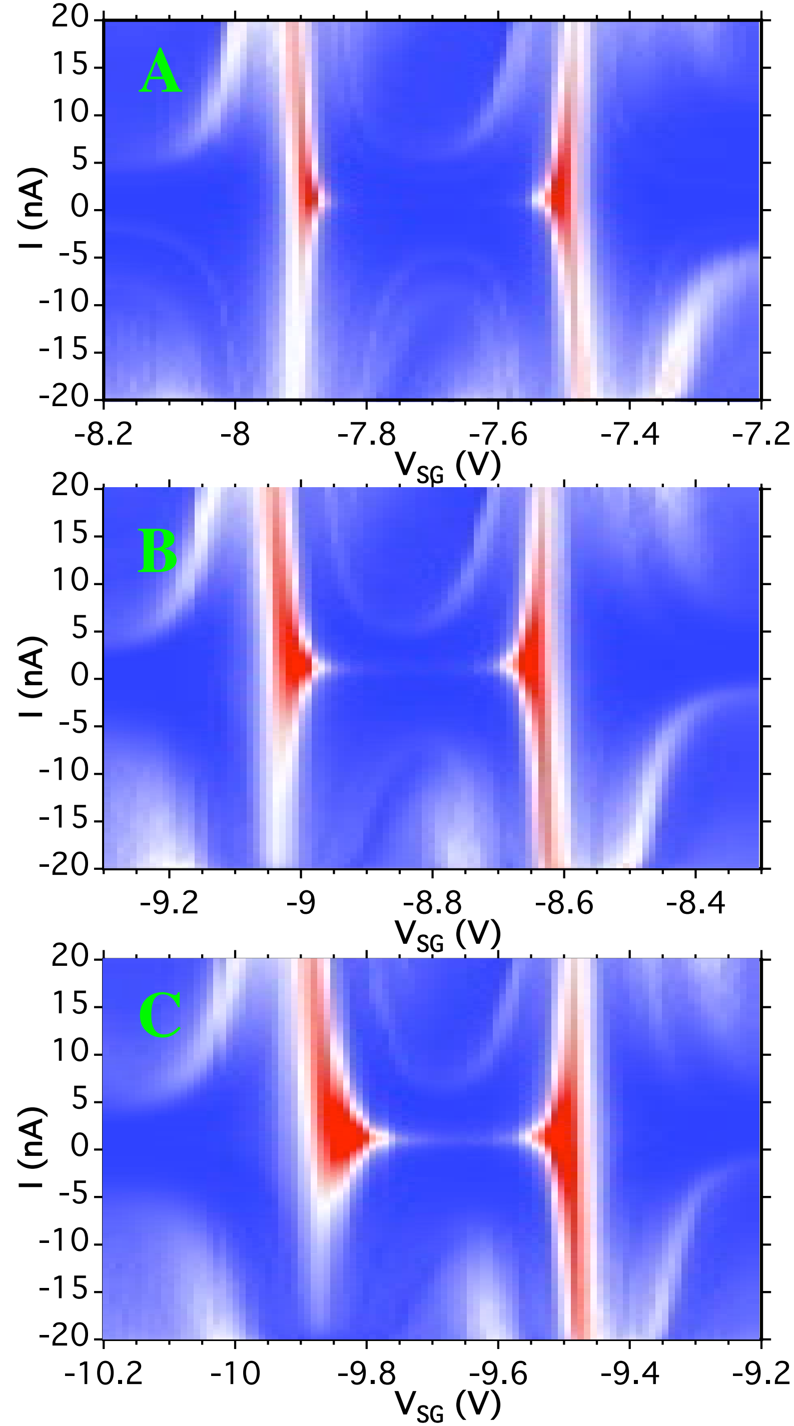

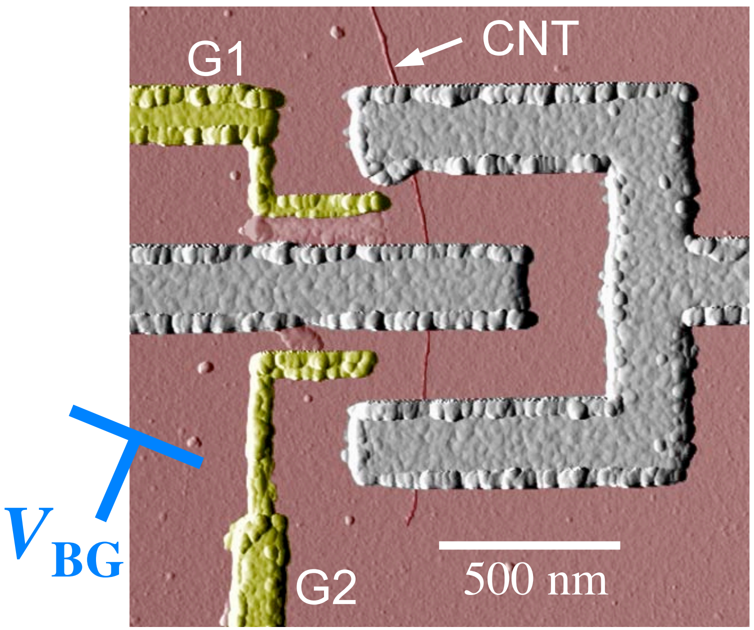

Carbon nanotube SQUID

$$I_c = \sqrt{(I_{c1} - I_{c2})^2 + 4 I_{c1} I_{c2} \cos^2(\pi \Phi_e / \Phi_0)}$$

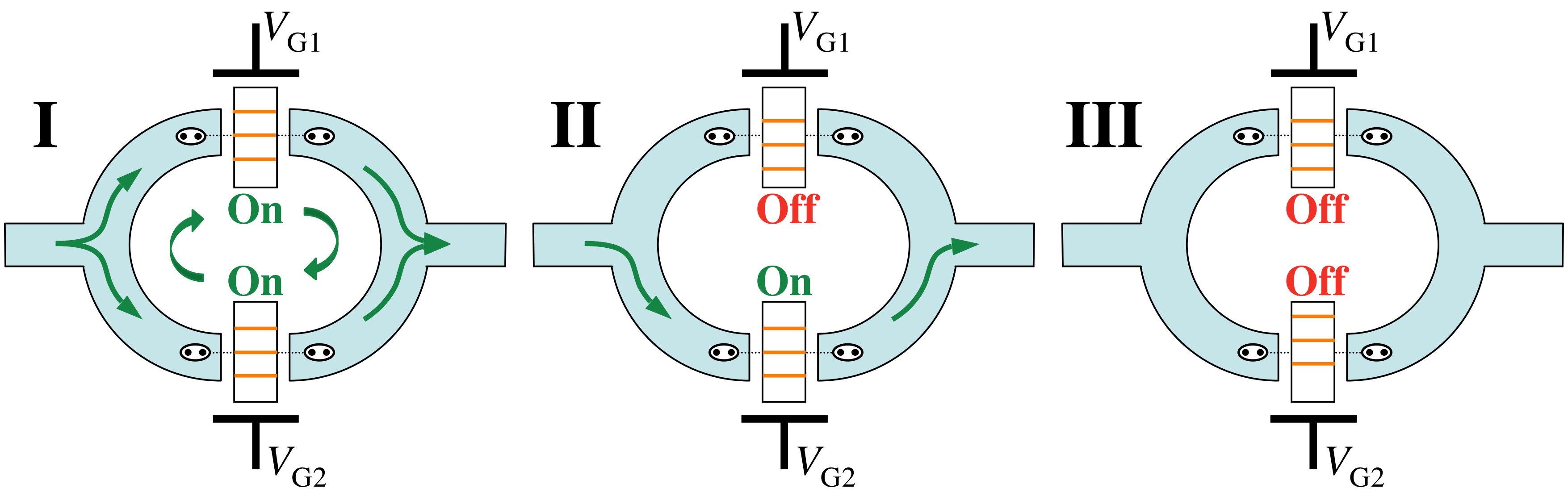

Differential conductivity *dI/dV* map versus sidegate voltages

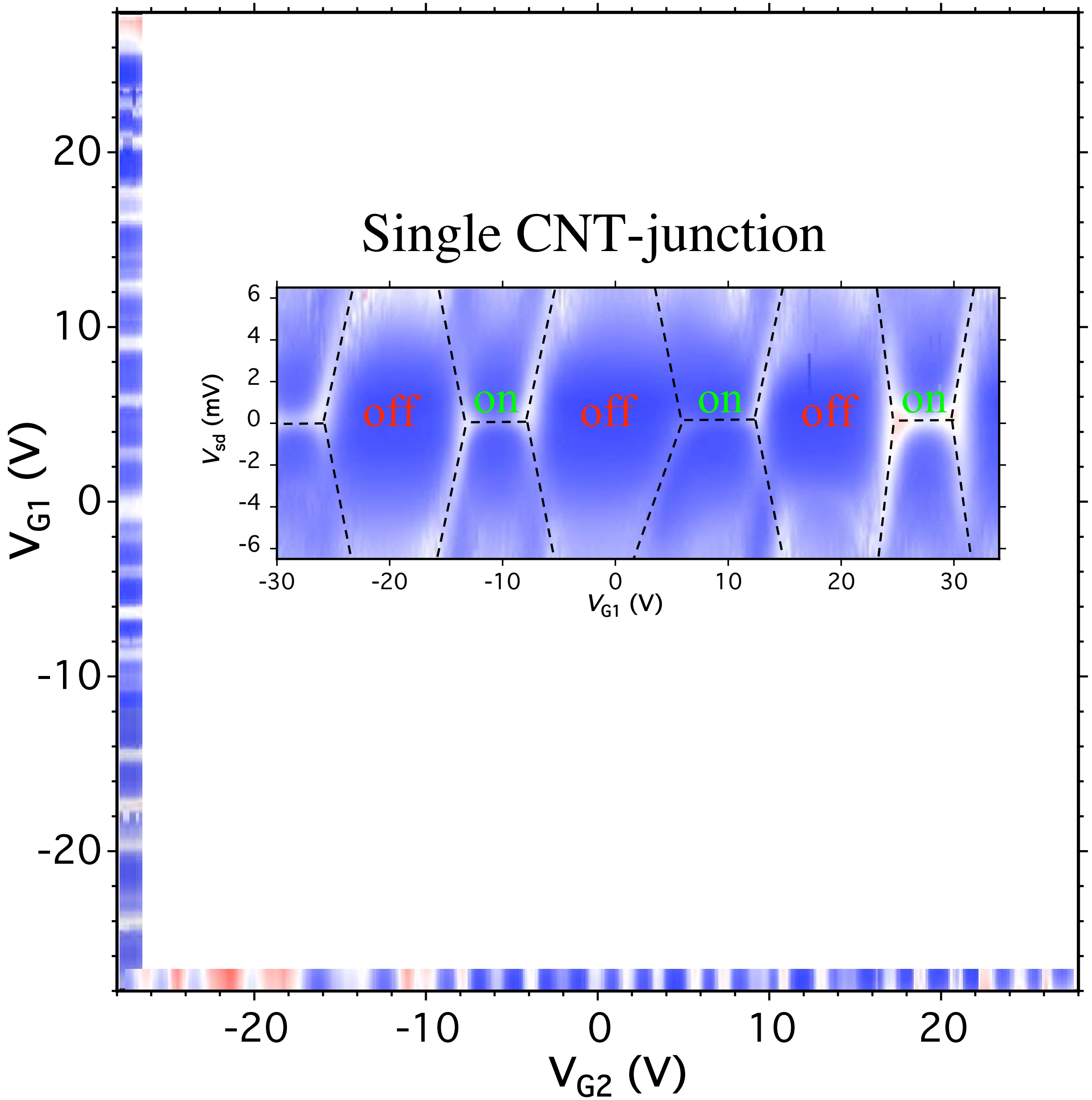

H_z = 50 mT
35 mK
V_{BG} = 0V
V_{SD} = 0V

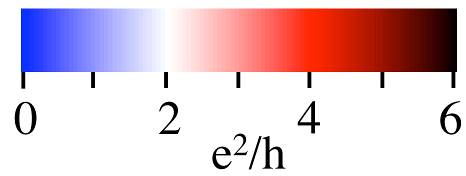

Differential conductivity *dI/dV* map versus sidegate voltages

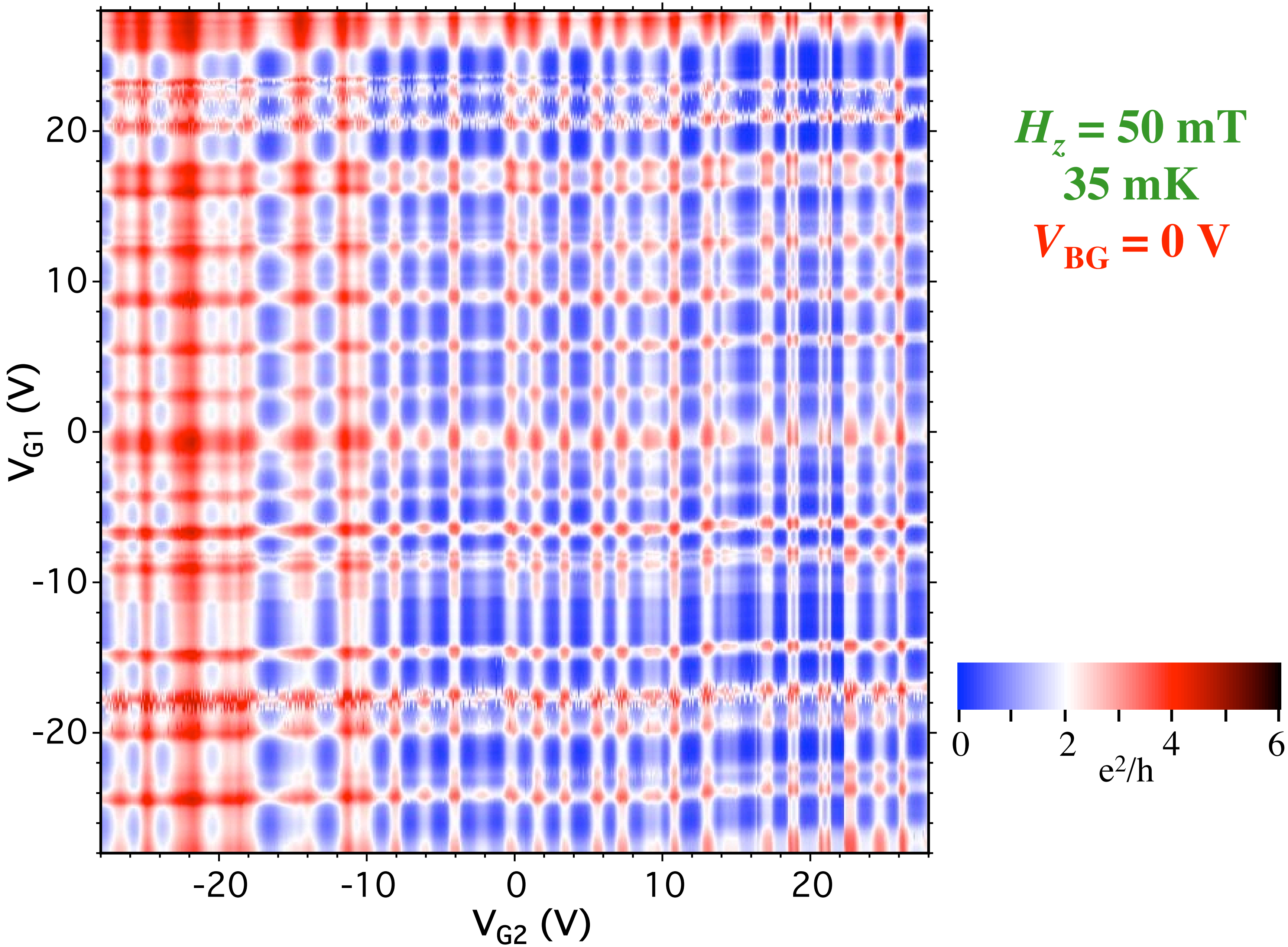

H_z = 50 mT
35 mK
V_{BG} = 0 V

Differential conductivity *dI*/*dV* map versus sidegate voltages

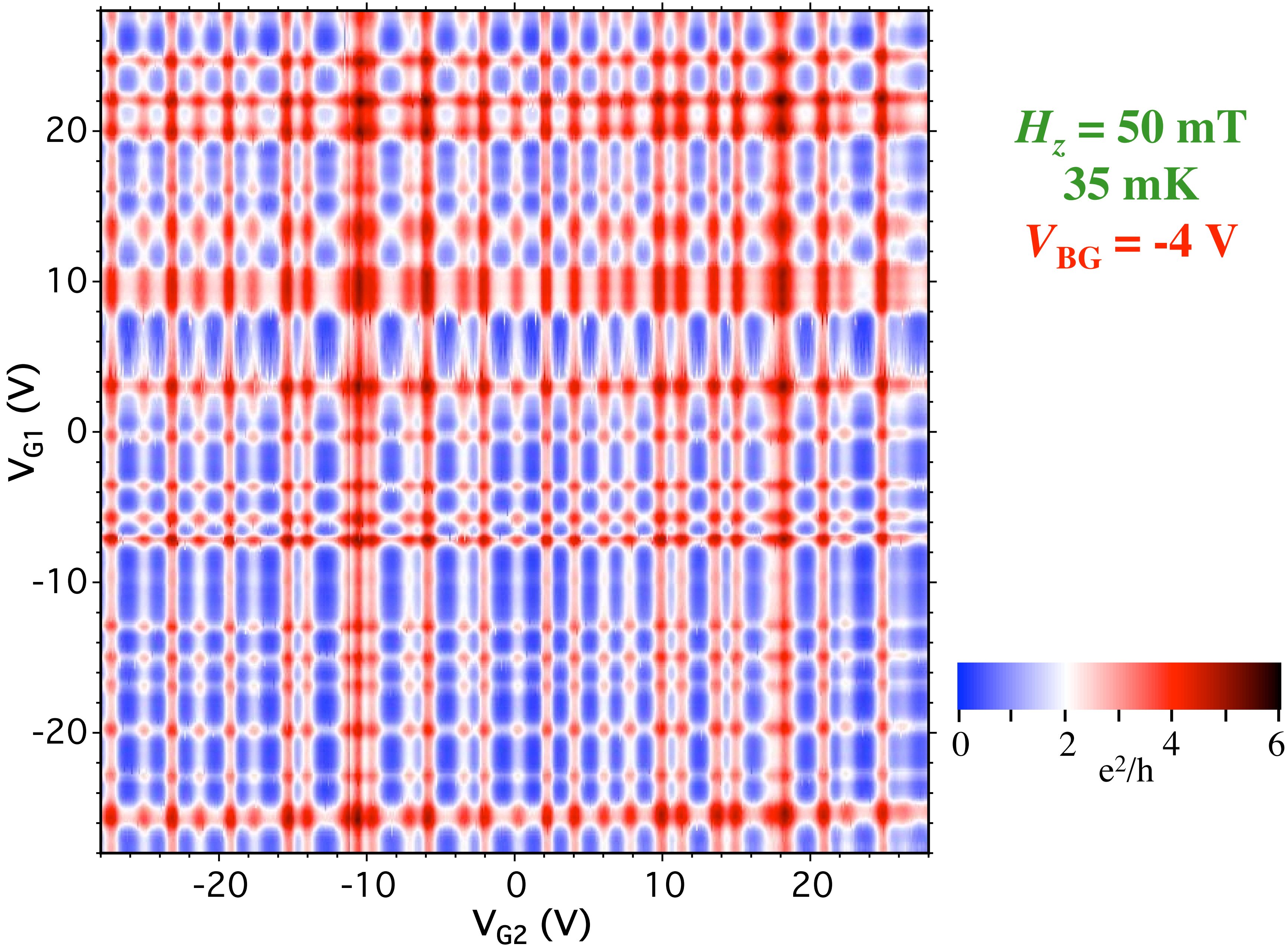

Correlation between normal state conductance and superconducting switching current I_{sw}

V_{BG} = -6V

$dI/dV(V_{G1},V_{G2})$ map
H_z = 50 mT

$I_{sw}(V_{G1},V_{G2})$ map
H_z = 0

$I_{sw}(V_{G1},V_{G2})$ map
H_z = 1.3 mT
($\Phi_0/2=h/4e$)

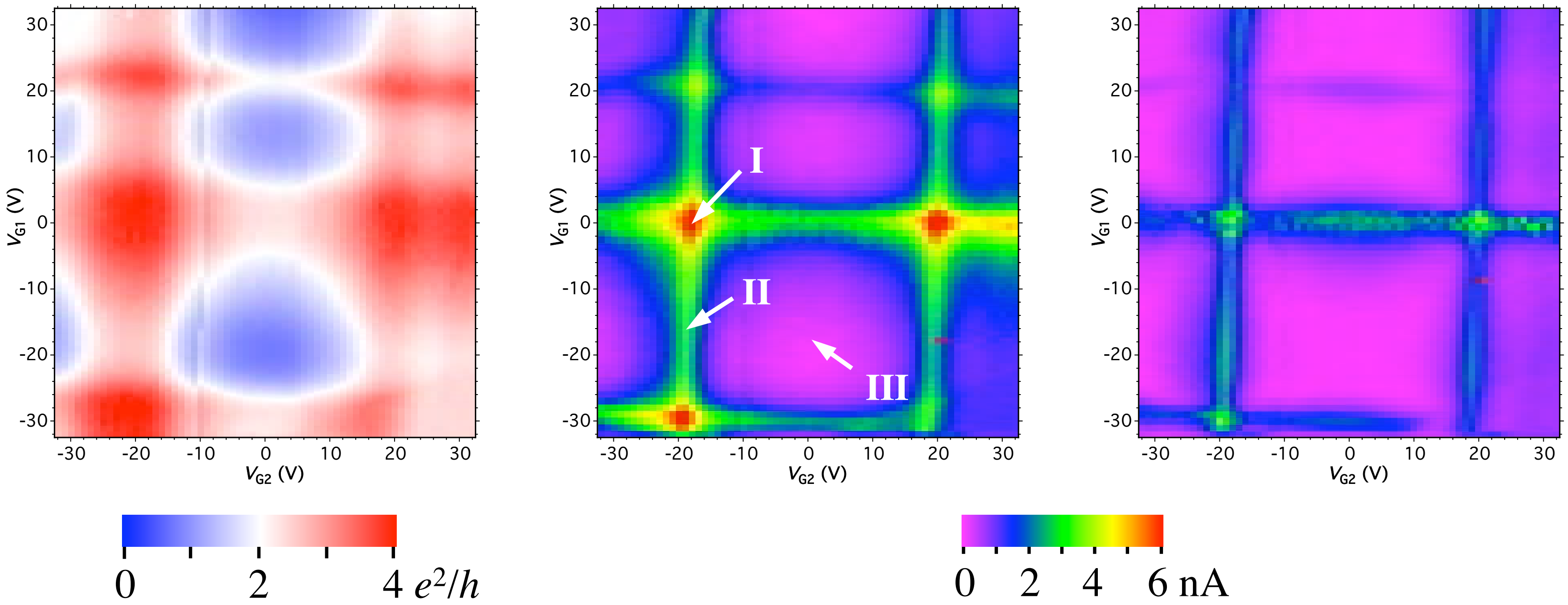

CNT-SQUID characteristics

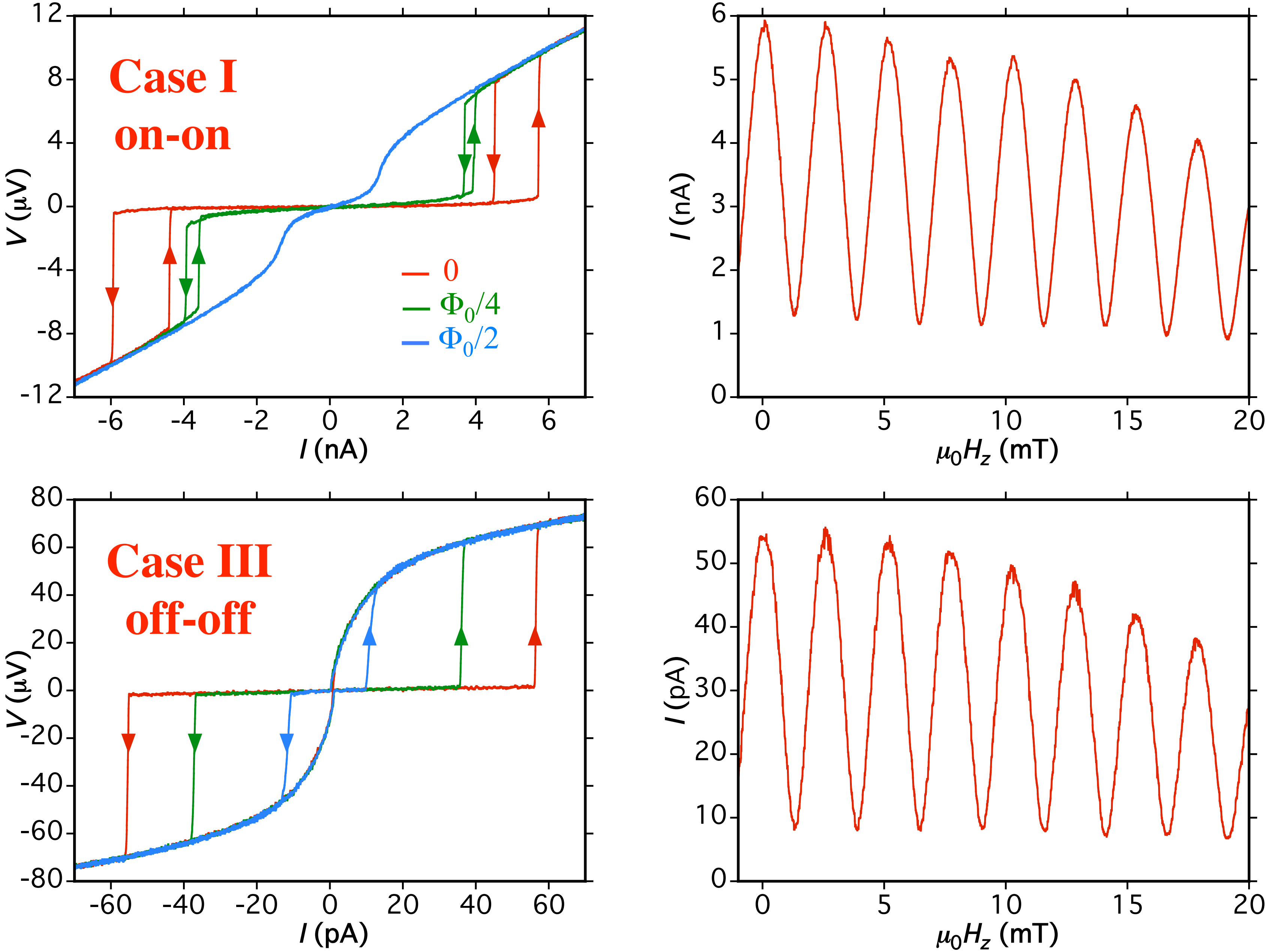

π - junction SQUID

$dI/dV(V_{G1},V_{G2})$ map
H_z = 50 mT

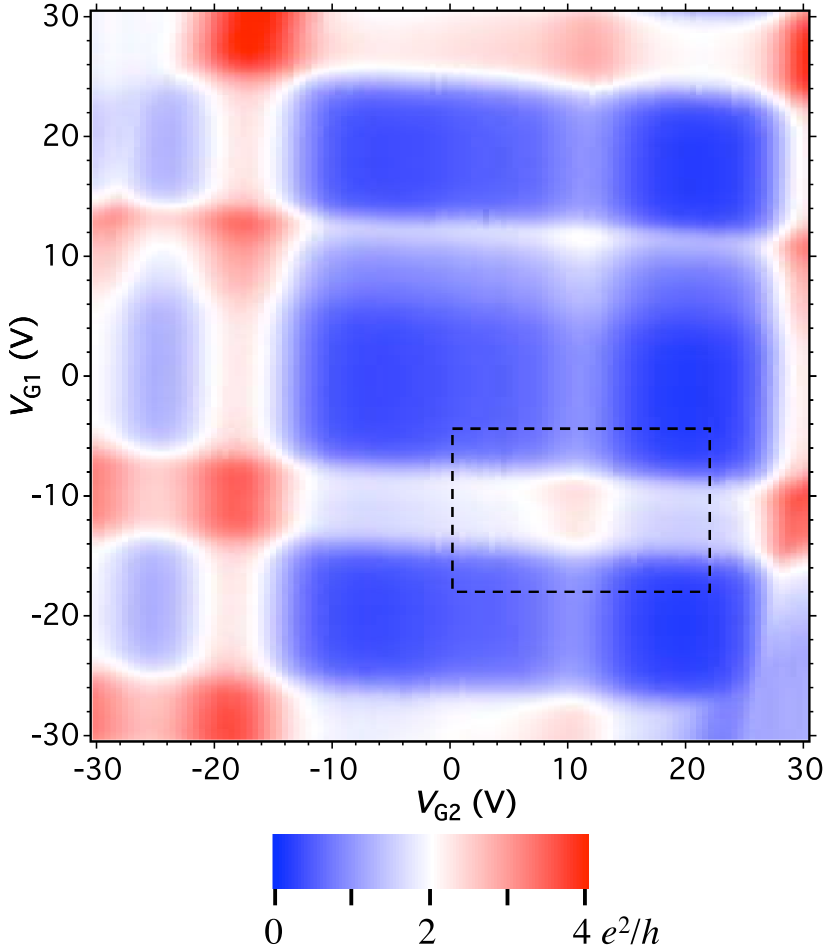

$I_{sw}(V_{G1},V_{G2})$ map
H_z = 0

V_{BG} = 0 V

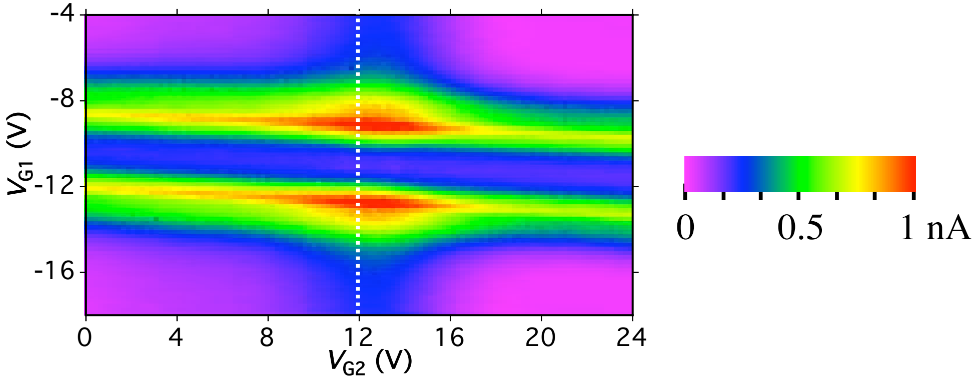

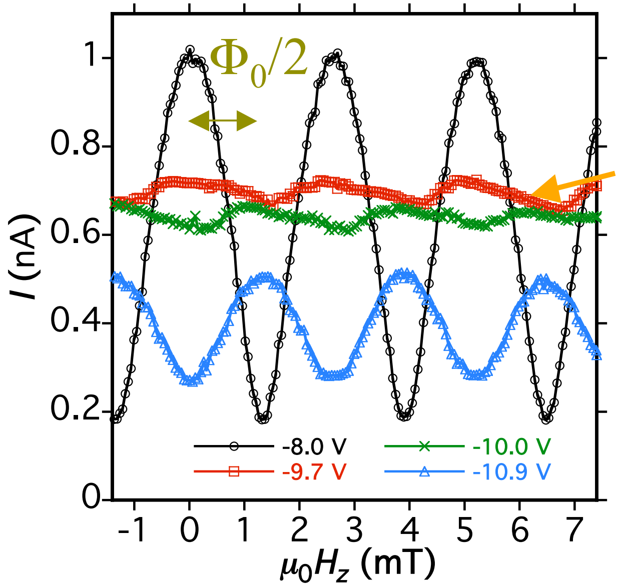

Current-phase relation NOT sinusoidal

π - junction SQUID

$dI/dV(V_{G1},V_{G2})$ map

H_z = 50 mT

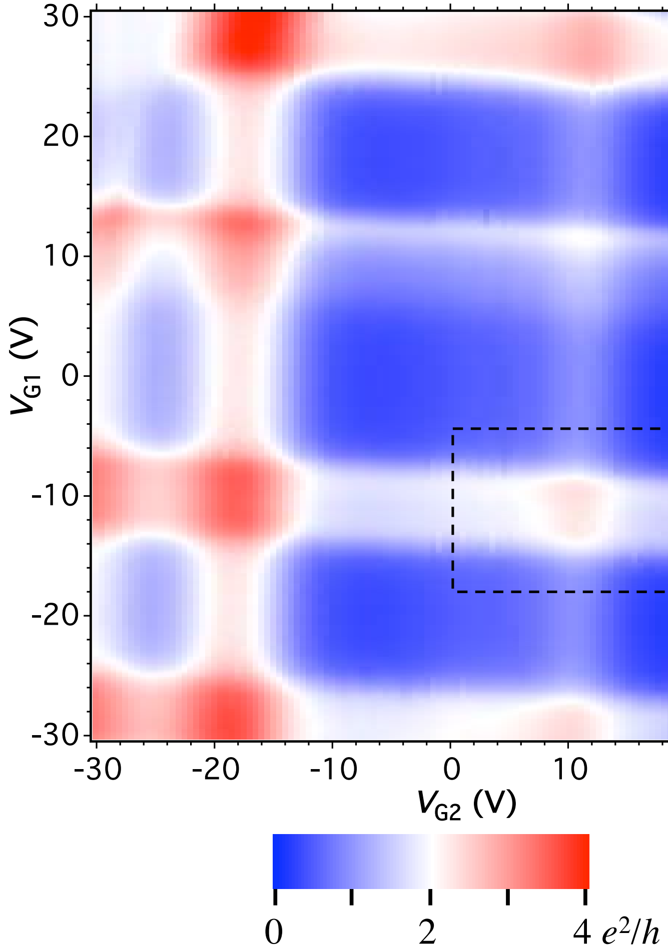

$I_{sw}(V_{G1},V_{G2})$ map V_{BG} = 0 V

H_z = 0

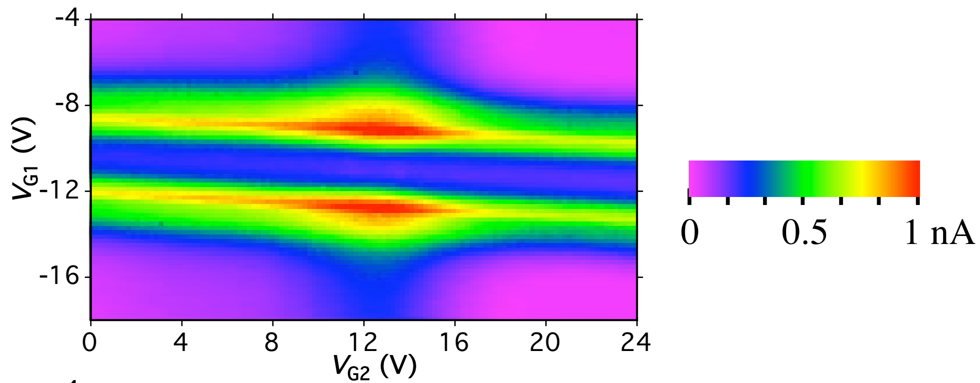

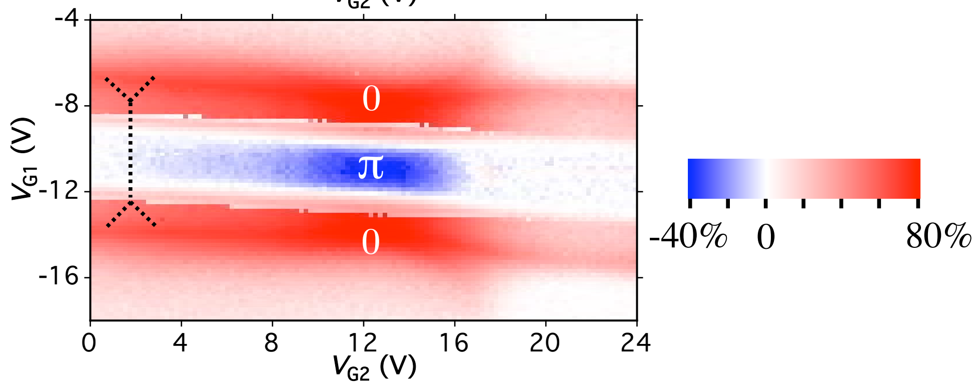

0 = |cos| flux modulations

π = |sin| flux modulations

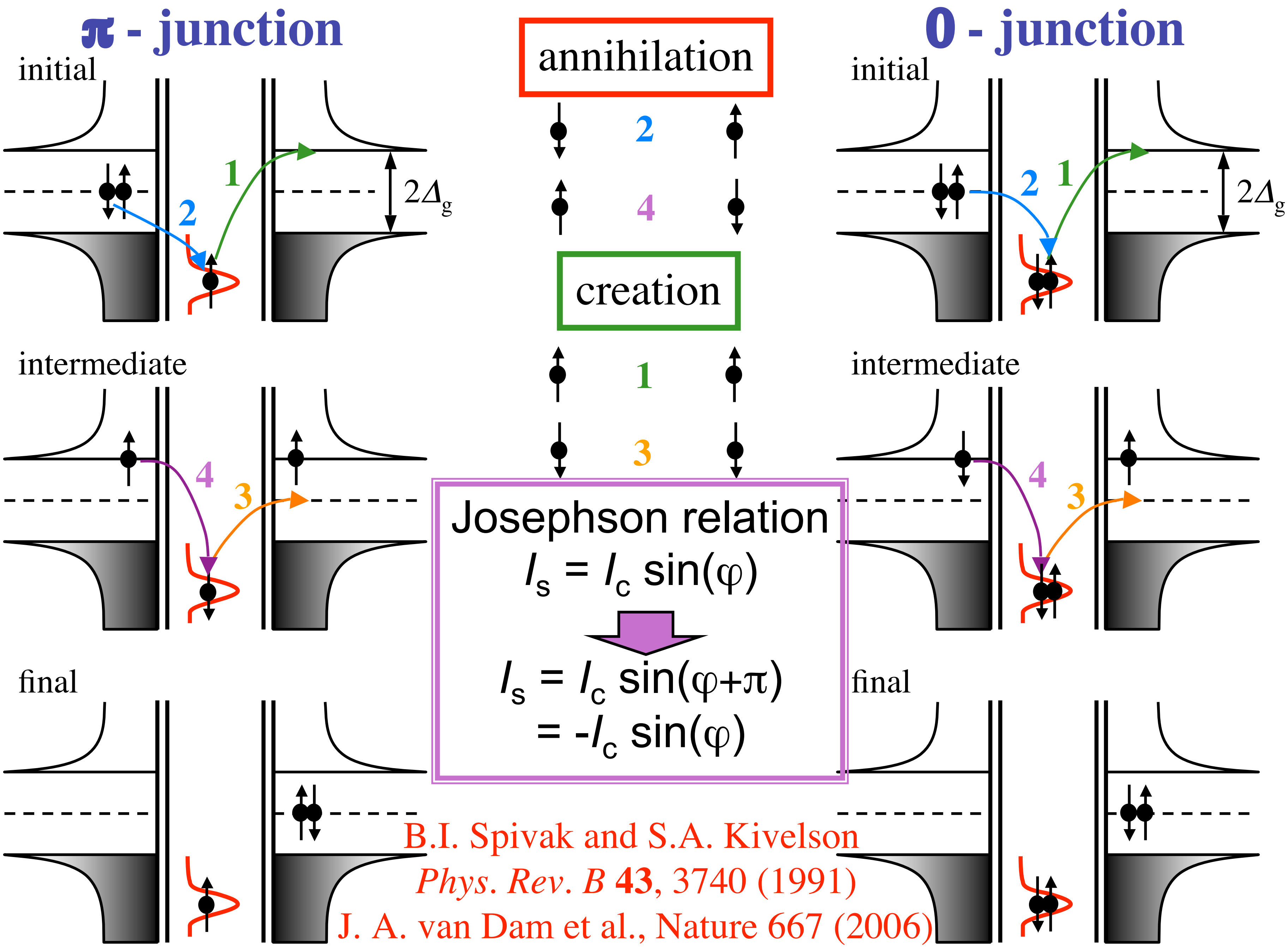
π - junction
initial
intermediate
final
1
2
3
4
$2\Delta_g$
annihilation
2
4
creation
1
3
0 - junction
initial
intermediate
final
1
2
3
4
$2\Delta_g$
Josephson relation
$I_s = I_c \sin(\varphi)$
$I_s = I_c \sin(\varphi+\pi)$
$= -I_c \sin(\varphi)$
B.I. Spivak and S.A. Kivelson
Phys. Rev. B **43**, 3740 (1991)
J. A. van Dam et al., Nature 667 (2006)

Double π-junction SQUID

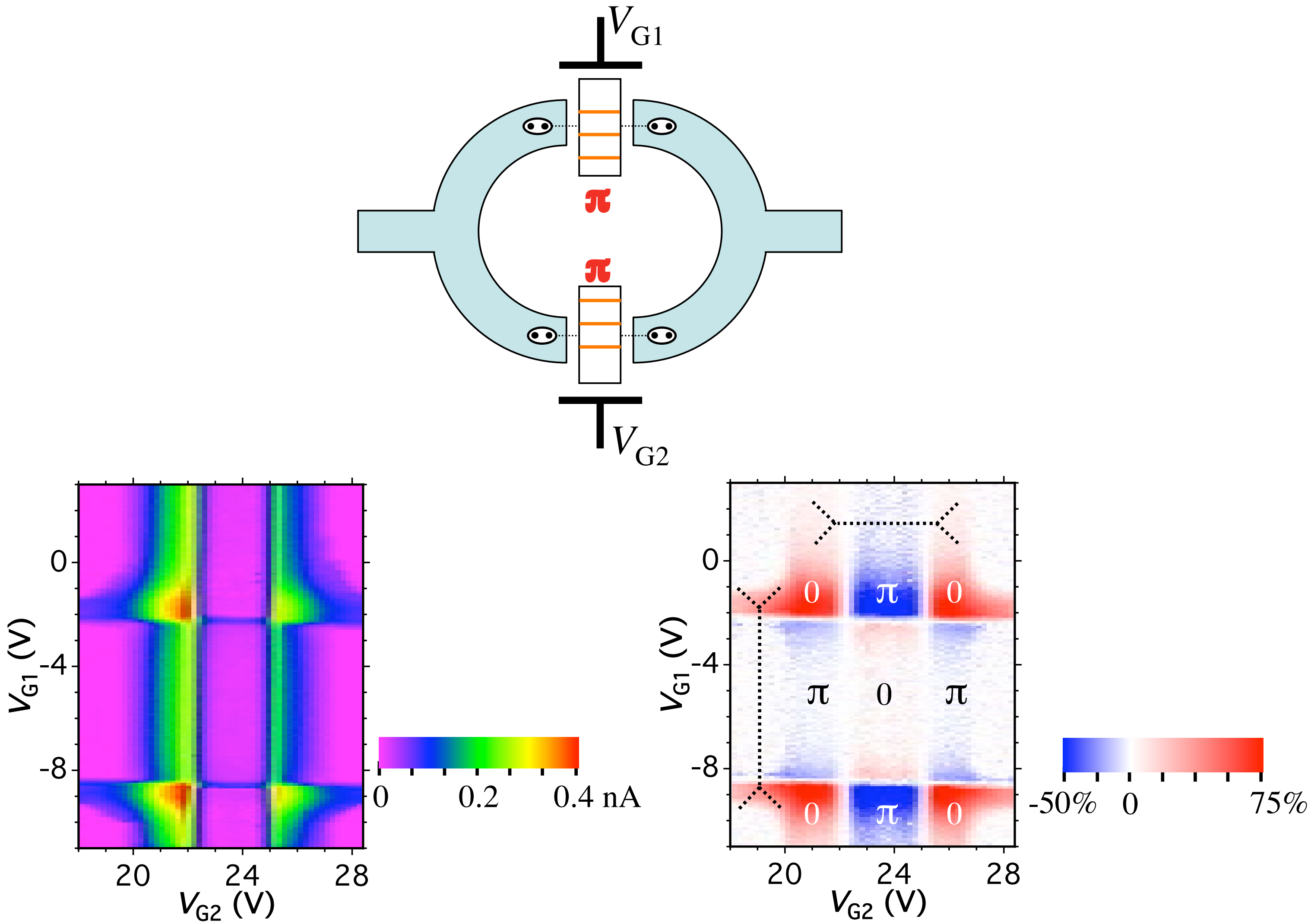

Preliminary estimation of the flux sensitivity of CNT-SQUIDs

CNT-SQUID characteristics

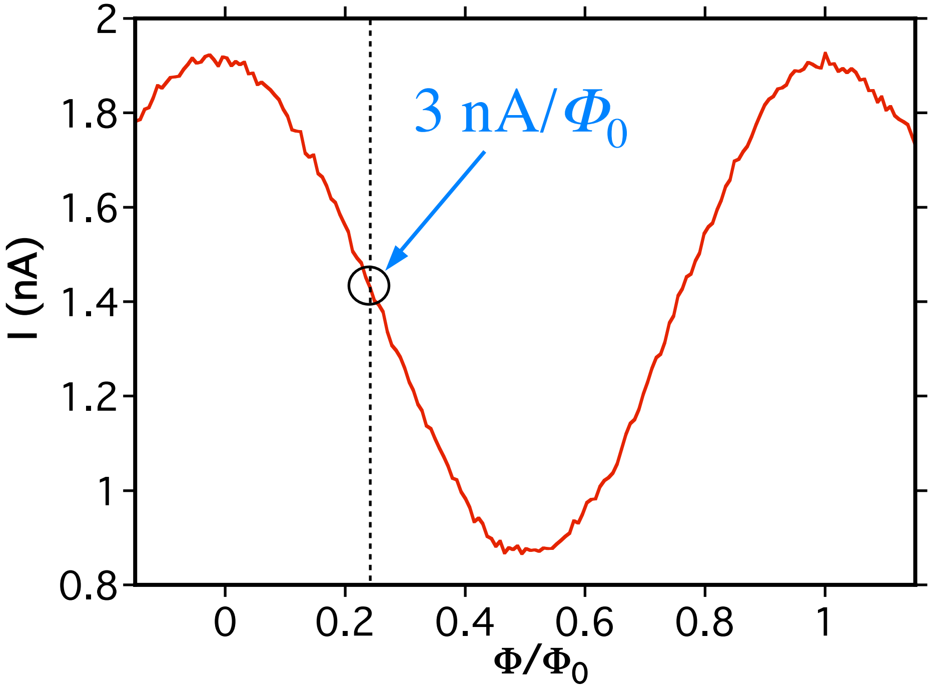

I_{sw} histogram

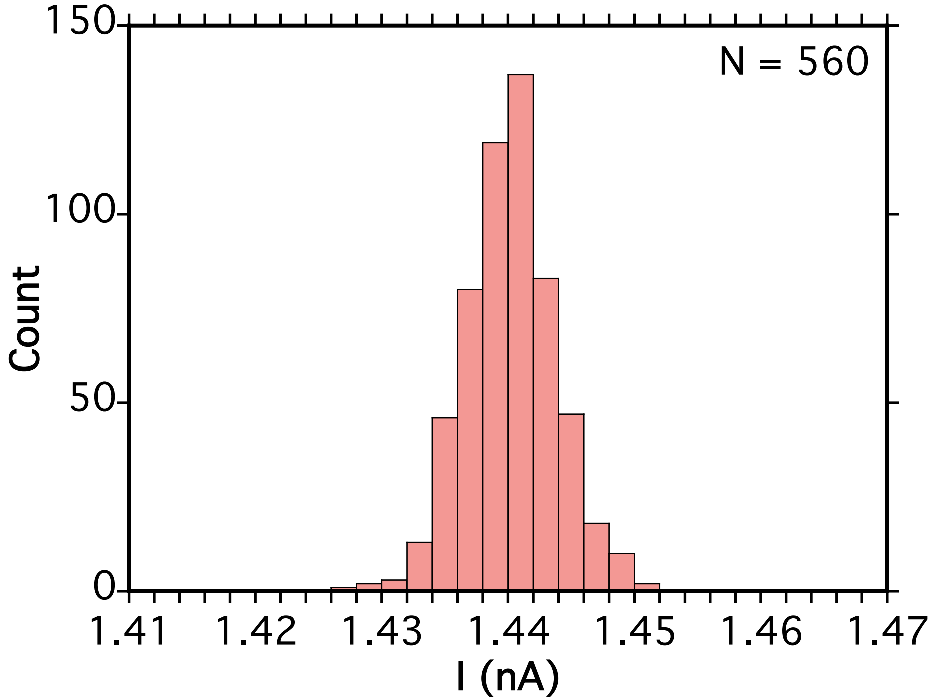

Flux sensitivity: [3.5 pA]/([3 nA/Φ_0]*sqrt[10000]) ≈ **10^{-5} Φ_0**
when averaging I_{sw} during 1 s at a rate of 10 kHz.

Estimation of magnetic flux variation for Mn_{12} with S = 10

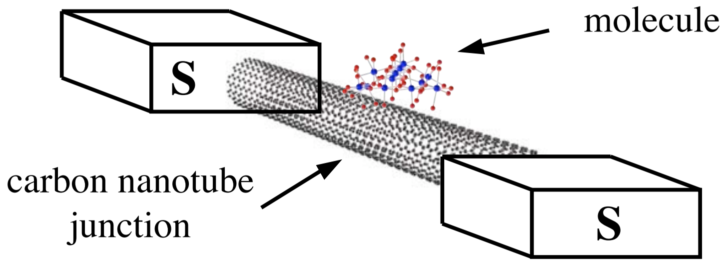

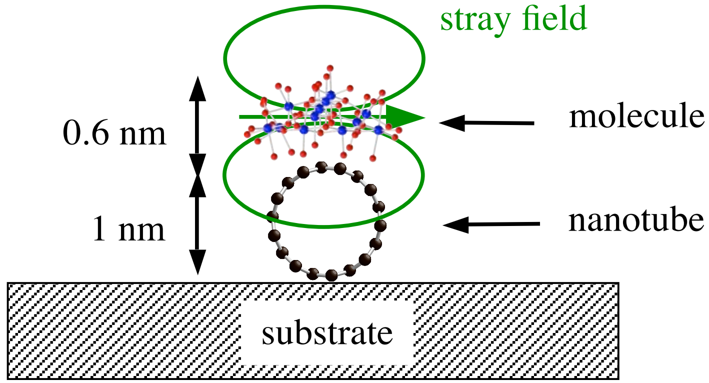

The total magnetic flux Φ of a uniformly magnetized sphere, $R = 0.5$ nm.

$$\boxed{\Phi = \frac{1}{2}\mu_0 \frac{m}{R}}$$

$\Delta\Phi = 1.1 \times 10^{-4}\ \Phi_0$ for Mn_{12} with S = 10

Flux sensitivity for the CNT-SQUIDs: $10^{-5}\ \Phi_0$
when averaging I_{sw} during 1 s at a rate of 10 kHz

further improvement, Irfan Siddiqi, Berkeley

I_{ac} - dependence of V(I) (Shapiro steps)

"on" - state

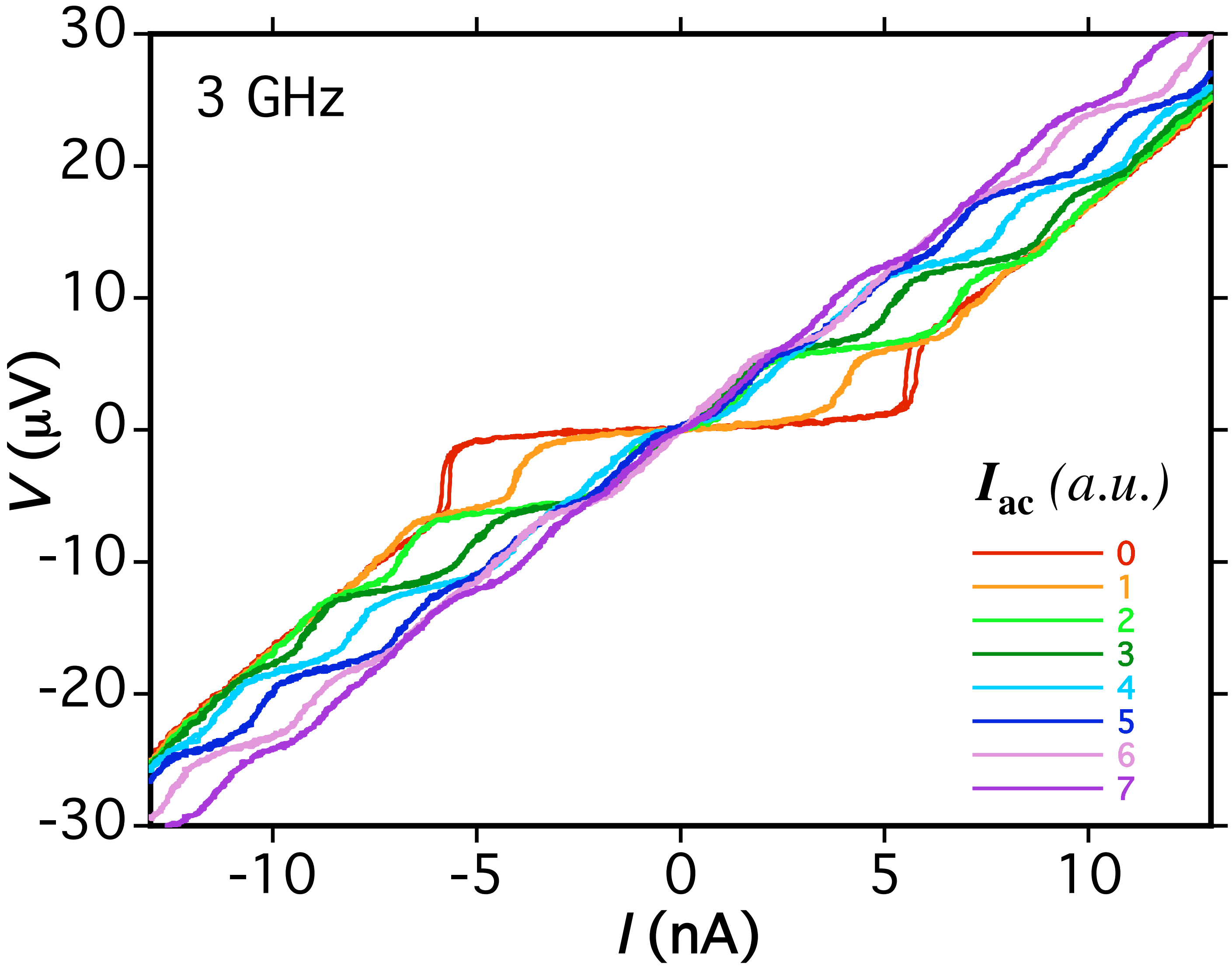

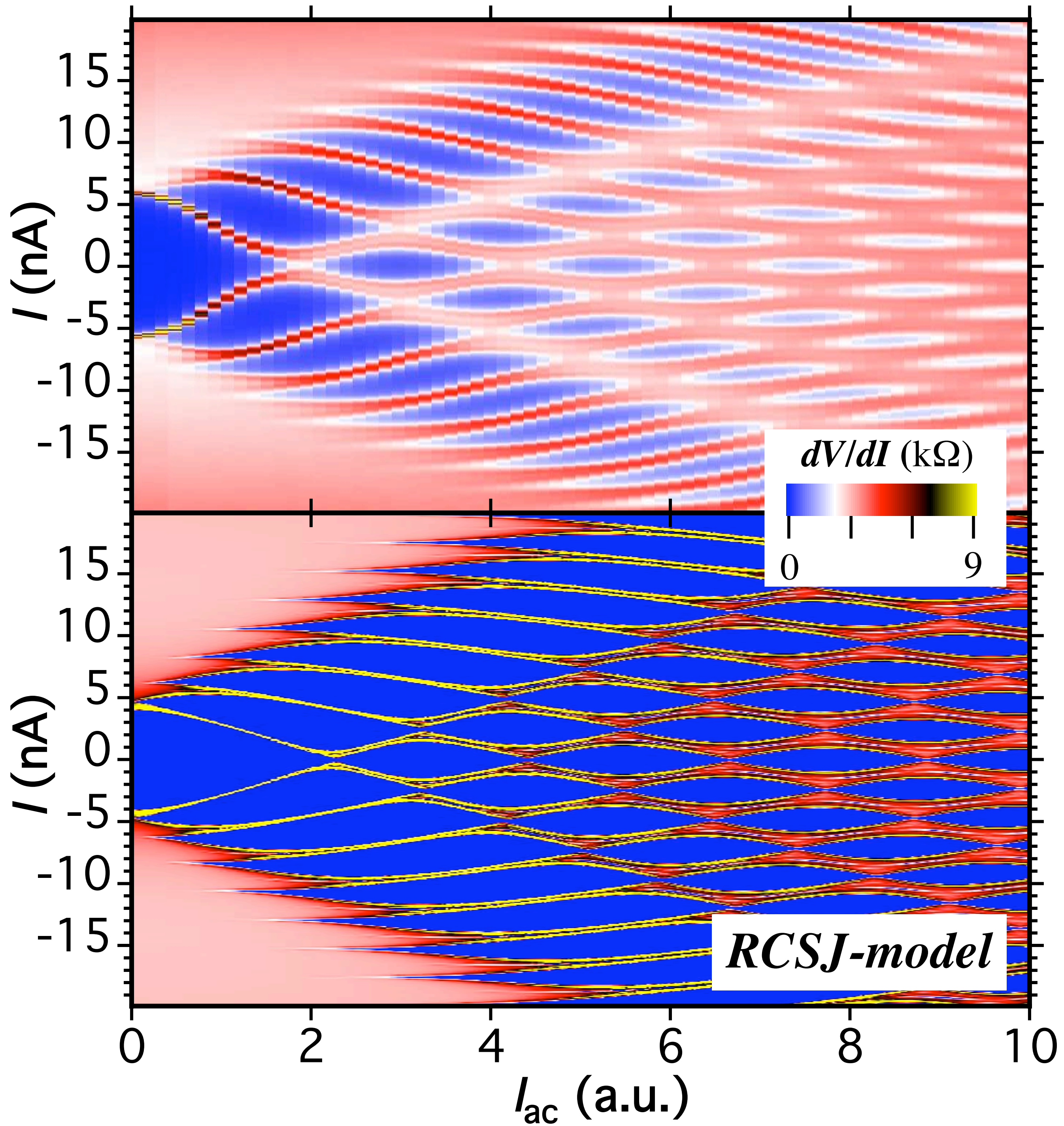

High frequency response

Shapiro steps

“on” - state

***C* = 30 aF**

Cont-mat/0705.2033

I_{ac} - dependence of V(I) (Shapiro steps)
"off" - state

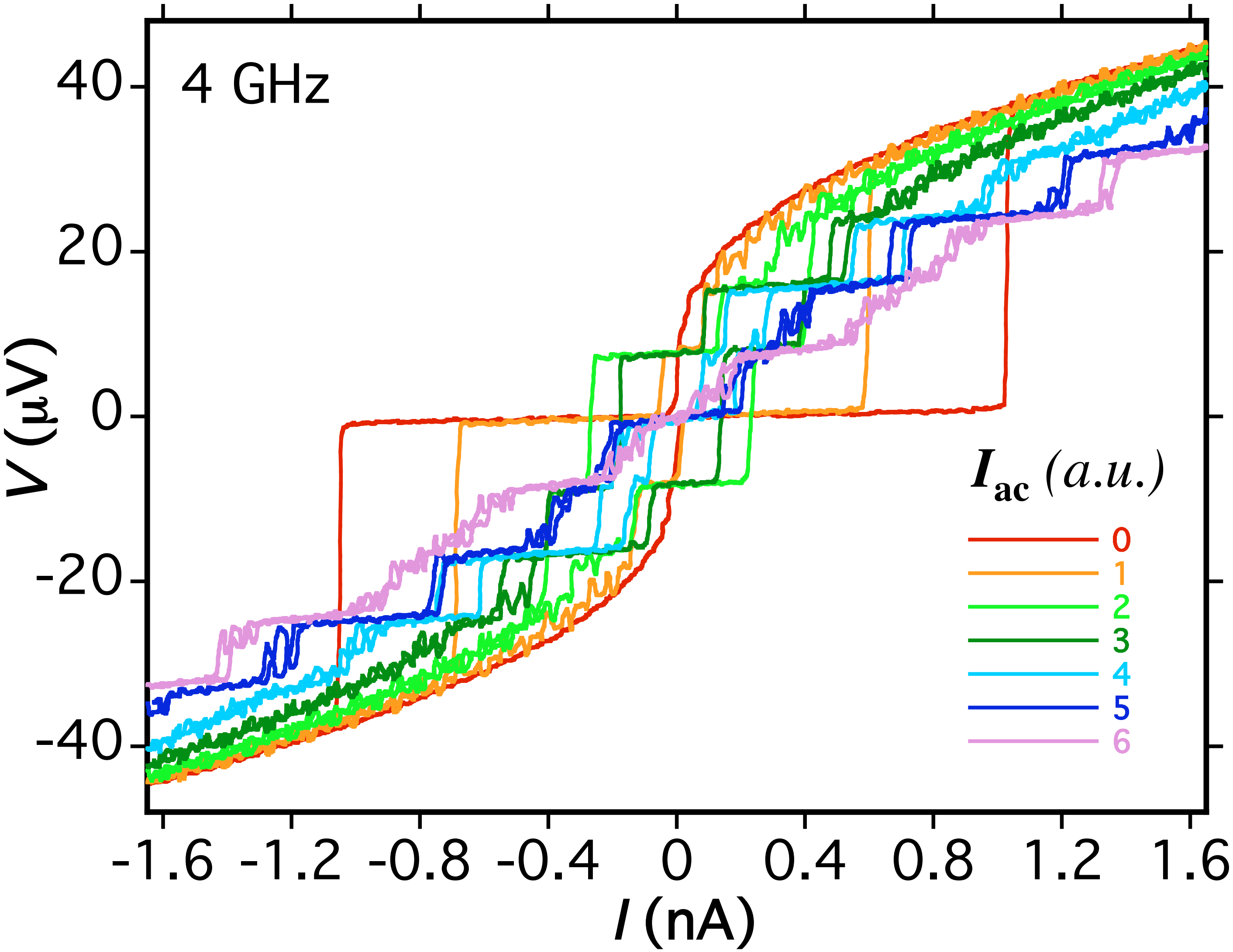

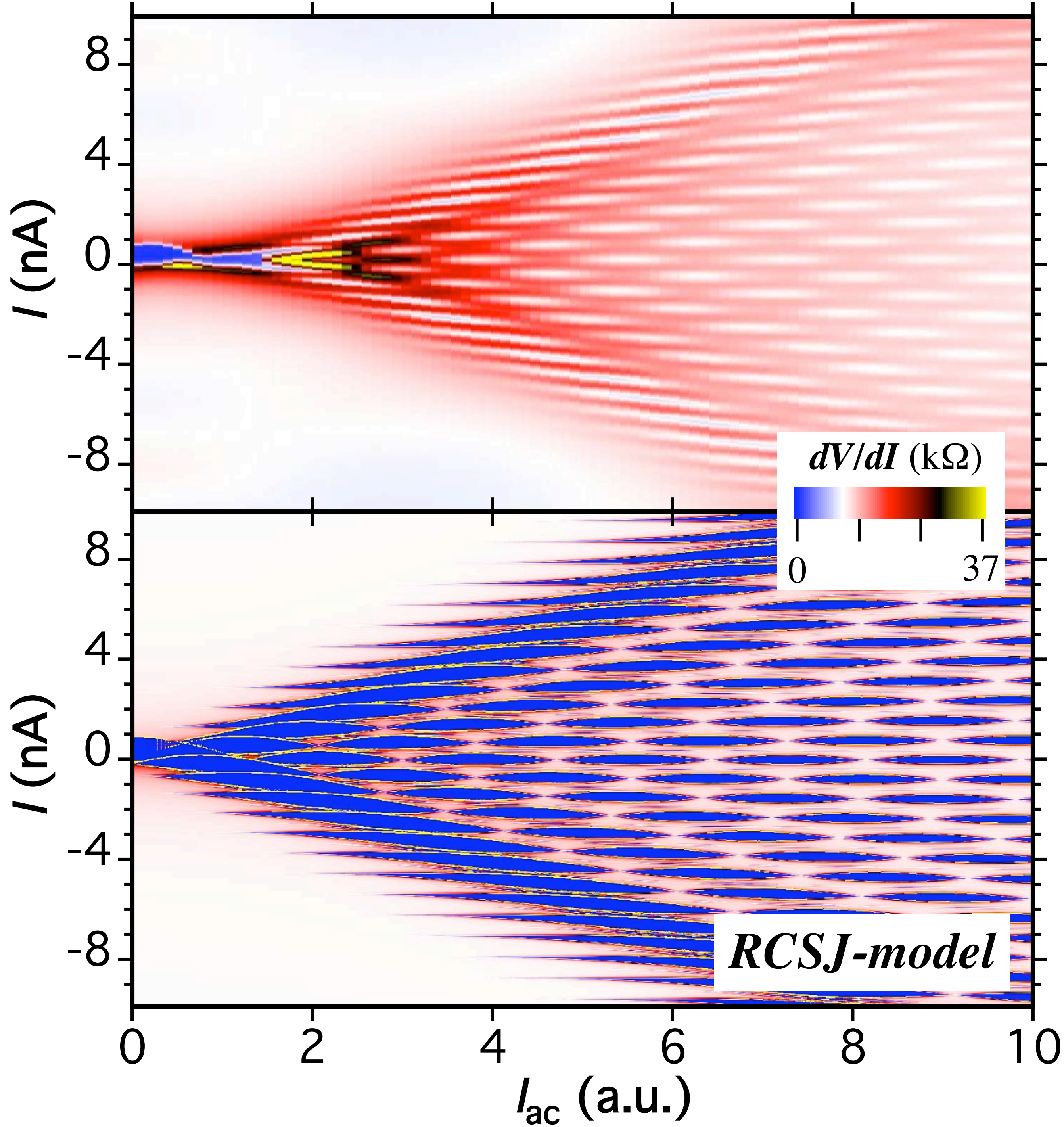

High frequency response

Shapiro steps

“off” - state

C = 1 fF

Cont-mat/0705.2033

Molecular spintronics

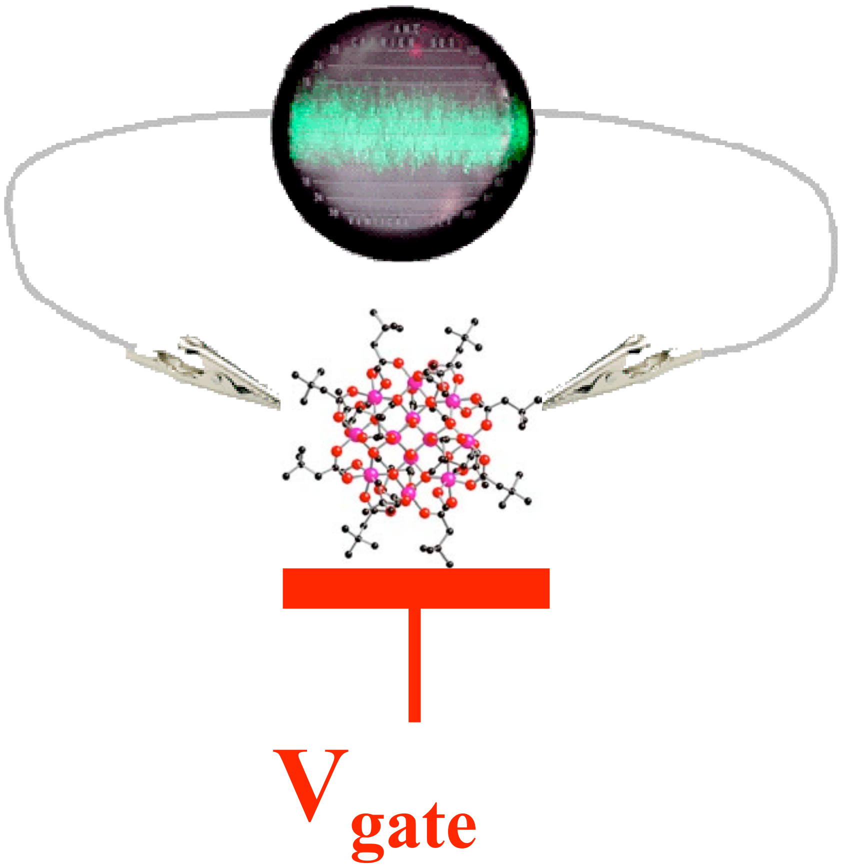

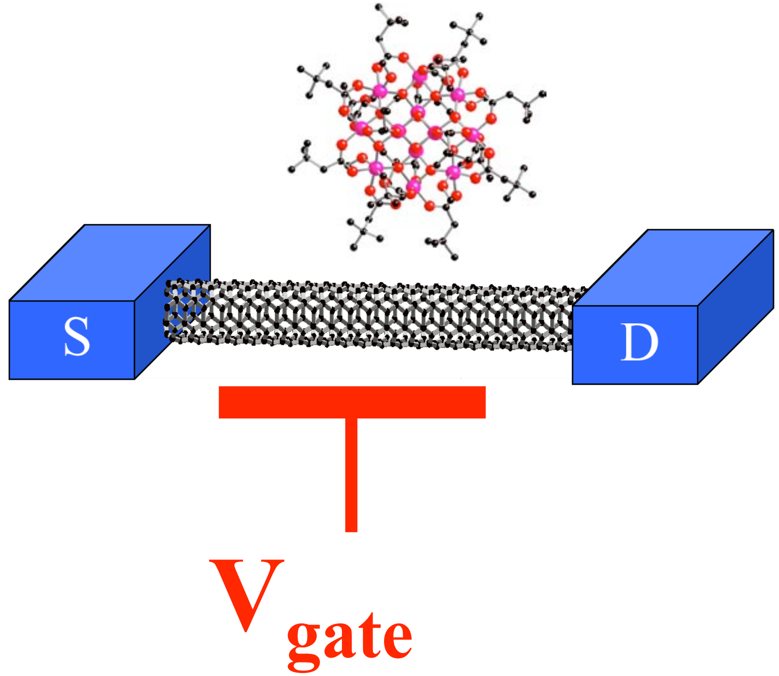

Nicolas Roch, Franck Balestro, Edgar Bonet
Cecile Delacour, Clemens Winkelmann, Romain Maurand, Lapo Bogani,
Laetitia Marty, Vincent Bouchiat, Wolfgang Wernsdorfer

Acknowledgement

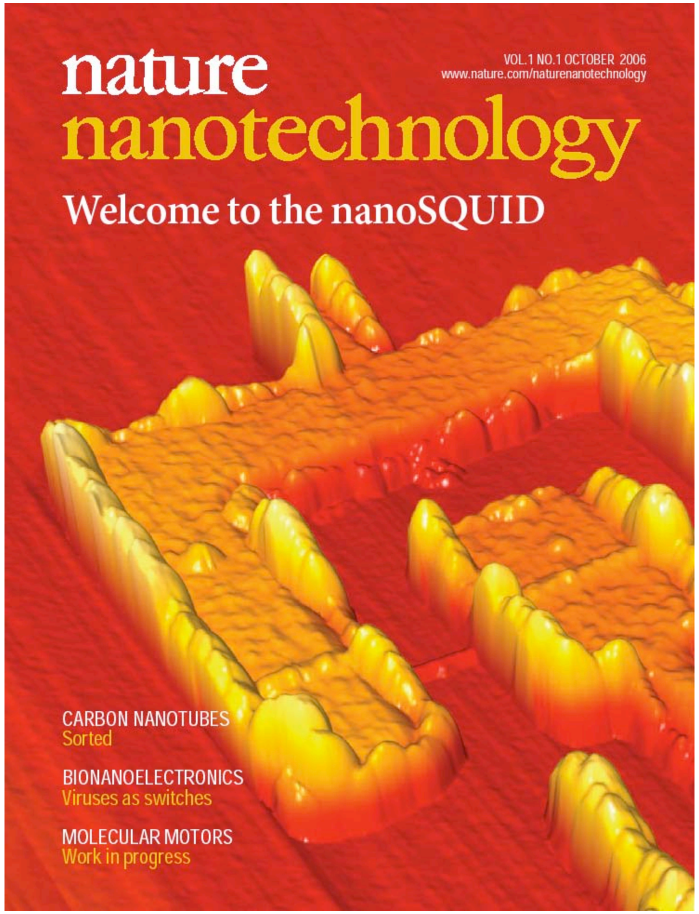

J.-P. Cleuziou, W. Wernsdorfer,
V. Bouchiat, Th. Ondarçuhu,
M. Monthioux

Nature Nanotechnology, 1, 53 (2006)

Theoretical support

Sabine Andergassen,

Serge Florens,

Denis Feinberg

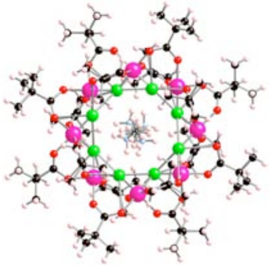

Winpenny, 2003

Collaborations (Chemistry)

SMMs

Group of G. Christou, Dept. of Chemistry, Florida
Group of R. Sessoli, D. Gatteschi, Univ. de Firenze, Italie
Group of A. Cornia, Univ. de Modena, Italie
Group of R.E.P. Winpenny, Univ. de Manchester, UK
Group of E. Brechin, Univ. de Manchester, UK
Group of T. Mallah, Orsay
Group of V. Marvaud, Univ. P. et M. Curie, Paris
Group of A. Müller, Univ. de Bielefeld, Germany
Group of A. Powell, Univ. de Kahlsruhe, Germany
Group of D. Hendrickson, Dept. of Chemistry, San Diego
Group of E. Coronado, Univ. de Valence, Spain
Group of D. Luneau, Univ. of Lyon, France
Group of G. Royal, Univ. J. Fourier, Grenoble

Mn_{84}

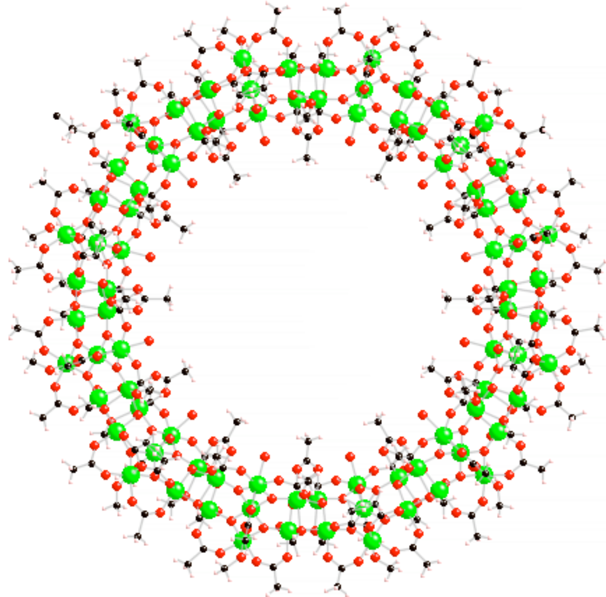

Christou, 2004

SCMs

Group of R. Clerac & C. Coulon, Univ. Bordeaux, Pessac
Group of H. Miyasaka, Tokyo Metropolitan Uni.
Group of M. Verdaguer, Univ. P. et M. Curie, Paris
Group of M. Julve, Univ. de Valence, Spain
• • •

MAGMANet NETWORK OF EXCELLENCE